BRN2 is a non-canonical melanoma tumor-suppressor

Michael Hamm, Pierre Sohier, Valérie Petit, Jérémy H Raymond, Véronique Delmas, Madeleine Le Coz, Franck Gesbert, Colin Kenny, Zackie Aktary, Marie Pouteaux, et al.

BRN2 is a non-canonical melanoma tumor-suppressor

Michael Hamm[1-3$], Pierre Sohier[1-3*$], Valérie Petit[1-3$], Jérémy H Raymond[1-3], Véronique Delmas[1-3], Madeleine Le Coz[1-3], Franck Gesbert[1-3], Colin Kenny[4], Zackie Aktary[1-3], Marie Pouteaux[1-3], Florian Rambow[1-3], Alain Sarasin[5], Nisamanee Charoenchon[1-3,6], Alfonso Bellacosa[7], Luis Sanchez-del-Campo[8], Laura Mosteo[8], Martin Lauss[9], Dies Meijer[10], Eirikur Steingrimsson[11], Göran B Jönsson[9], Robert A Cornell[4], Irwin Davidson[4,12], Colin R Goding[8#], and Lionel Larue[1-3#*]

(1) Institut Curie, Université PSL, CNRS UMR3347, Inserm U1021, Normal and Pathological Development of Melanocytes, 91400 Orsay, France
(2) Université Paris-Saclay, CNRS UMR3347, Inserm U1021, Signalisation radiobiologie et cancer, 91400 Orsay, France
(3) Equipes Labellisées Ligue Contre le Cancer
(4) Department of Anatomy and Cell biology, Carver College of Medicine, University of Iowa, Iowa City, IA 52242, USA
(5) Laboratory of Genetic Instability and Oncogenesis, UMR8200 CNRS, Gustave Roussy, Université Paris-Sud, Villejuif, France.
(6) Department of Pathobiology, Faculty of Science, Mahidol University, Bangkok, 10400, Thailand
(7) Cancer Epigenetics Program, Fox Chase Cancer Center, Philadelphia, PA, USA
(8) Ludwig Institute for Cancer Research, Nuffield Department of Clinical Medicine, University of Oxford, Headington, Oxford, OX3 7DQ, UK.
(9) Department of Oncology, Clinical Sciences Lund, Lund University and Skåne University Hospital, Lund, Sweden.
(10) Centre of neuroregeneration, University of Edinburgh, Edinburgh, United Kingdom
(11) Department of Biochemistry and Molecular Biology, and 5Department of Anatomy, BioMedical Center, Faculty of Medicine, University of Iceland, Sturlugata 8, 101 Reykjavik, Iceland
(12) Institut de Génétique et de Biologie Moléculaire et Cellulaire, CNRS/INSERM/UNISTRA, 1 Rue Laurent Fries, 67404 Illkirch Cedex, France. Department of Functional Genomics and Cancer.

$ These authors contributed equally to this study.
* Corresponding authors: Lionel Larue: lionel.larue@curie.fr
# co last authors: Colin Goding & Lionel Larue

The authors declare no potential conflicts of interest.

Running title: BRN2 is a tumor-suppressor

KEYWORDS

Melanoma; phenotypic switch; mouse molecular genetics; Haplo-insufficiency; human; Mitf; Cre-LoxP; tamoxifen; POU3F2

ABSTRACT (150 words)

While the major drivers of melanoma initiation, including activation of NRAS/BRAF and loss of *PTEN* or *CDKN2A*, have been identified, the role of key transcription factors that impose altered transcriptional states in response to deregulated signaling is not well understood. The POU domain transcription factor BRN2 is a key regulator of melanoma invasion, yet its role in melanoma initiation remains unknown. Here, in a $Braf^{V600E}$ $Pten^{F/+}$ context, we show that *BRN2* haplo-insufficiency promotes melanoma initiation and metastasis. However, metastatic colonization is less efficient in the absence of Brn2. Mechanistically, BRN2 directly induces *PTEN* expression and in consequence represses PI3K signaling. Moreover, MITF, a BRN2 target, represses *PTEN* transcription. Collectively, our results suggest that on a *PTEN* heterozygous background somatic deletion of one *BRN2* allele and temporal regulation of the other allele elicits melanoma initiation and progression.

INTRODUCTION

Cancer initiation is triggered by the activation of oncogenic signaling combined with senescence bypass. Yet while many typical oncogenes and tumor suppressors that affect cancer initiation have been identified, cancer initiation is likely to be modulated by additional genetic events. Understanding how non-classical driver mutations may impact cancer initiation is a key issue that has been relatively underexplored. Melanoma, a highly aggressive skin cancer, arises through the acquisition of well-defined genetic and epigenetic modifications in oncogenes and tumor suppressors and represents an excellent model system to address this key question.

As a highly genetically unstable cancer type, the initiation of melanoma requires the induction of melanocyte proliferation, which is mediated by several major founder mutations, the most common of which are *BRAF*^{V600E} and *NRAS*$^{Q61K/R}$ [1,2]. However, activation of BRAF or NRAS is insufficient to promote melanoma initiation without senescence bypass mediated by additional founder mutations or expression changes of several genes including *p16*^{INK4A}, *CTNNB1*, *PTEN*, or *MDM4* [3-7].

The transcription factor BRN2, also known as POU3F2 and N-OCT3, plays a critical role in neurogenesis and drives proliferation in a range of cancer types with neural or neuroendocrine origins, including glioblastoma, neuroblastoma, small cell lung cancer, and neuroendocrine prostate cancer [8-10]. In the melanocyte lineage, BRN2 is not detected in melanoblasts *in vivo* but is heterogeneously expressed in naevi and melanoma [11-14]. *In vitro* studies have shown that BRN2 expression is induced by a range of melanoma-associated signaling pathways including activation of the mitogen-activated protein kinase (MAPK) pathway downstream from BRAF, the PI3K pathway, the LEF-β-catenin axis, as well as FGF, TNF-α, EDN3 and SCF

signaling [14-17]. Consistent with BRN2 being expressed in a predominantly mutually exclusive pattern with the Microphthalmia-associated transcription factor (MITF) [13] that plays a crucial role in melanoma proliferation [18], BRN2 is repressed by MITF via miR-211 [19]. However, the relationship between MITF and BRN2 is complex. For example, BRN2 was recently found to be regulated by E2F1, a cell cycle-regulated transcription factor that is also a target for MITF, and both BRN2 and MITF are regulated by PAX3 and WNT/β-catenin [15,16,20-24]. Indeed, both BRN2 and MITF can regulate expression of AXL [21,25], with BRN2 repressing AXL expression, thus enabling some cells in human melanoma to adopt an AXL^{High}, $MITF^{Low}$ and $BRN2^{Low}$ state [25]. The activation of BRN2 expression in a specific subset of melanoma cells in response to all three major signaling pathways (MAPK, PI3K/PTEN, and β-catenin) linked to melanoma initiation (early proliferation and bypass/escape senescence) and progression (including late proliferation and metastatic dissemmination) suggests that Brn2 is likely to have a critical role in disease progression [26]. Most notably, BRN2 has been associated with $MITF^{Low}$ senescent or slow-cycling cells [11], and identified as a key regulator of melanoma invasion and anoikis *in vitro* [13,27,28] and in *in vivo* xenograft experiments [20,29,30]. Mechanistically, the ability of BRN2 to promote invasion has been linked to its ability to control expression of PDE5A-mediated cell contractility, phosphorylation of myosin light chain 2, repression of MITF and PAX3, and cooperation with bi-allelic loss of CDKN2A [13,20,27,30]. However, despite abundant information linking BRN2 to melanoma proliferation and invasiveness *in vitro* and in xenograft experiments, the impact of BRN2 on melanoma initiation and progression *in vivo* has never been assessed.

In this work, we show that BRN2 acts as a tumor suppressor during melanoma initiation and progression in a *BRAF-PTEN* context since BRN2 and MITF regulate positively and negatively the transcription of *PTEN*, respectively.

RESULTS

BRN2 loss or low expression correlates with reduced survival and worse prognosis. Although BRN2 has been implicated in melanoma invasiveness, and its expression is highly regulated, whether and how it may contribute to melanoma initiation or incidence is not understood. To evaluate the prevalence of *BRN2* loss in human skin cutaneous melanoma (SKCM), we retrieved copy-number alteration (CNA) data for *BRN2* in SKCM metastases (stage IV) from the Cancer Genome Atlas (TCGA, https://cancergenome.nih.gov/). The *BRN2* locus showed mono-allelic loss in 53% and bi-allelic loss in 2.7% of all patient samples (n = 367, Figure 1A). Only a minority (n = 29 of 367, corresponding to 7.9%) of SKCM samples showed a copy-number gain (n = 27)/amplification (n = 2) for *BRN2*. We did not further analyze these samples since the expression of BRN2 was slightly increased but not statistically different (p=0.26, test of Kruskall-Wallis with a Dunn correction) between tumors that gained and/or amplified this locus compared to the normal situation. We screened a panel of human melanoma cell lines available in our laboratory (n = 23) for deletions that affect the *BRN2* locus by comparative genomic hybridization. The *BRN2* locus showed mono-allelic loss in 48% (11 out 23) of the human melanoma cell lines and no bi-allelic loss, comparable to the TCGA-data (Supplementary Fig. 1A, Supplementary Data 1). Notably, BRN2 mRNA levels were significantly lower in SKCM metastases with bi-allelic BRN2 loss (Supplementary Fig. 1B). The mono- and bi-allelic loss of *BRN2* was frequently associated with a large segmental deletion of the long arm of chromosome 6 (Chr.6q) in SKCM metastases and in our cell line panel (Figure 1B, Supplementary Fig. 1C, Supplementary Data 2). From the TCGA,

patients carrying the monoallelic loss of *BRN2* in metastases displayed a trend to have a shorter overall survival than those with diploid status (Figure 1C). These results were validated using an independent cohort of 118 regional metastases previously described [31] (Figure 1D). Moreover, we evaluated the number of BRN2 alleles in nevi and melanoma that arose from these nevi using publically available data [32]. It appears that 28% (5 out of 18) or 22% (4 out of 18) of melanomas presented either a mono-allelic loss or a gain of *BRN2* respectively compared to nevi (Supplementary Fig. 1D). The situation is clearly complex, but we may conclude that *BRN2* mono-allelic loss can occur during the early steps of melanomagenesis.

We next assessed the correlation between BRN2 mRNA levels and overall patient survival to evaluate the effect of *BRN2* mono-allelic loss on melanoma progression. We established “BRN2-high” and “BRN2-low” patient groups based on RNA-seq data available from the TCGA (BRN2 subgroups defined as BRN2-low (≤ 1 transcript per million reads [TPM]) and BRN2 expressed/high [> 1 TPM]). Patients in the “BRN2-low” group displayed significantly shorter overall survival than those of the “BRN2-high” group (Figure 1E). Overall, the *BRN2* locus*,* frequently associated with a large segmental deletion, is lost (mono- and bi-allelic) in ≈60% of human SKCM metastases and correlates with significantly reduced overall survival. Since *CCNC*, *ROS1* and *ARID1B* loci are distal to *BRN2* on chromosome 6, and are known to be involved in melanomagenesis, we evaluated the overall survival of these patients according to the presence and the level of mRNA expression of the corresponding genes. We observed no significant difference between the presence or absence of these three genes or their expression (Supplementary Fig. 1E-L). Finally, we compared the loss of 6q with the mono-allelic loss (MAL) of *BRN2* (Supplementary

Fig. 1M) and found that 6q loss is associated with a worse prognostic than *BRN2* mono-allelic loss. This result indicates, as suspected, that other gene(s) located on 6q are of importance in melanomagenesis. Taken together, these data indicate that in human melanoma BRN2 loss/low expression is associated with an adverse outcome for the patient.

Co-occurrence of *BRN2* loss with mono-allelic loss of *PTEN*

We next determined whether BRN2 loss co-occurs with melanoma driver mutations by examining the TCGA CNA-data set and human melanoma cell-line panel. There was no significant correlation between *BRAF* or *NRAS* mutation and *BRN2* loss (mono- or bi-allelic), neither in human melanoma samples nor the human cell-line panel (Supplementary Fig. 2A,B). We then searched for co-occurring CNAs of other known melanoma-associated genes and found that mono-allelic loss of *BRN2* co-occurred with mono-allelic loss of *PTEN* in approximately 40% of the human melanoma samples in TCGA and in the human cell-line panel (Supplementary Fig. 2C,D). We next evaluated the concomitant *BRN2* locus alterations, *BRAF*/*NRAS* mutations, and *CDKN2A*/*PTEN* alterations and found the most frequent genetic constellation that co-occurs with *BRN2* loss in melanoma to be $BRAF^{V600X}$ mutation together with mono-allelic *PTEN* loss (Supplementary Fig. 2E). Finally, we compared the overall survival of human patients with a loss of one allele of *PTEN* who also had a loss of *BRN2* (monoallelic loss = MAL) with a loss of one allele of *PTEN* and no loss of *BRN2* (BRN2-normal). In this context, patients with loss of *BRN2* showed significantly lower overall survival than *BRN2*-normal patients (Supplementary Fig. 1N).

In conclusion, in human melanoma, the loss of *BRN2* is preferentially associated with *BRAF* mutation together with *PTEN* loss.

Loss of *BRN2* drives melanomagenesis *in vivo.*

These data suggesting that the loss of *BRN2* might be of importance in melanoma prompted us to evaluate the potential causal role of BRN2 in melanomagenesis *in vivo* by examining whether heterozygous (het) or homozygous (hom) loss of *Brn2* affects melanoma initiation and/or progression in a mouse model. Note however, that while genetic loss of BRN2 might be important, the complex regulation of BRN2 expression driven by melanoma-associated signaling pathways might also play a major role, especially given that melanoma cells within a single tumor can exhibit both high and very low BRN2 expression [13,20]. We therefore developed an inducible genetically engineered mouse model system for generating Brn2-deficient melanoma driven by the most common alterations in human SKCM ($Braf^{V600E}$ and *Pten* loss). Specifically, we used $Tyr::Cre^{ERt2/+-Lar}$; $Braf^{V600E/+}$ (called Braf from hereon) and $Tyr::Cre^{ERt2/+-Lar}$; $Braf^{V600E/+}$; $Pten^{F/+}$ (called Braf-Pten from hereon) mice carrying a tamoxifen-inducible Cre-recombinase under the control of the tyrosinase promoter [33-35]. This model system allows melanocyte lineage-specific induction of a $BRAF^{V600E}$ mutation and mono-allelic deletion of *Pten* for Braf-Pten mice. Cre-mediated defloxing leads to activation of the $Braf^{V600E}$ oncogene, inducing nevus and spontaneous melanoma formation in Braf mice, reproducing many of the cardinal histological and molecular features of human melanoma [36]. Bi-allelic and mono-allelic

loss of *PTEN* reduces tumor latency in $Braf^{V600E}$- and $NRAS^{Q61K}$-driven mouse melanoma models [3,37].

Using these models, we studied the effect of Brn2 insufficiency (het and hom) on *in vivo* melanomagenesis by introducing the floxed Brn2 locus into the genome by appropriate crossings (Supplementary Fig. 3A) [38]. Specifically, we generated the mouse lines *Tyr::Cre$^{ERT2/°}$; Braf$^{V600E/+}$*; *Brn2$^{+/+}$* (Braf-Brn2-WT), *Tyr::Cre$^{ERT2/°}$; Braf$^{V600E/+}$*; *Brn2$^{F/+}$* (Braf-Brn2-het), *Tyr::Cre$^{ERT2/°}$; Braf$^{V600E/+}$*; *Brn2$^{F/F}$* (Braf-Brn2-hom), *Tyr::Cre$^{ERt2/°}$; Braf$^{V600E/+}$; Pten$^{F/+}$; Brn2$^{+/+}$* (Braf-Pten-Brn2-WT), *Tyr::Cre$^{ERt2/°}$; Braf$^{V600E/+}$; Pten$^{F/+}$; Brn2$^{F/+}$* (Braf-Pten-Brn2-het) and *Tyr::Cre$^{ERt2/°}$; Braf$^{V600E/+}$; Pten$^{F/+}$; Brn2$^{F/F}$* (Braf-Pten-Brn2-hom). Cre-mediated defloxing of *Braf*, *Pten*, and *Brn2* loci was induced by topical application of tamoxifen during the first three days after birth (Supplementary Fig. 3B). All mice were monitored for the appearance and growth rate of the first tumor, as well as for the number of tumors/mouse. Note that the ability to generate either homo- or heterozygous Brn2 KOs will mimic not only mono or biallelic loss in humans, but also reflect the variable levels of BRN2 observed within human tumors [13,20]. In the absence of PTEN (*Pten$^{F/F}$*) on a $Braf^{V600E}$ background, the appearance of the tumors was too rapid to observe any difference between Brn2 +/+, Brn2 F/+ or Brn2 F/F mice.

Braf-Brn2-WT/het/hom mice showed no differences in the appearance of the first tumor, number of tumors/mouse or the tumor growth rate from those of Braf-WT mice (Figure 2, Supplementary Fig. 3C). However, compared to Braf-Pten-Brn2-WT, Braf-Pten-Brn2-het/hom mice significantly increased the number of tumors/mouse and the tumor growth rate, but not the timing of the appearance of the first tumor (Figure 2, Supplementary Fig. 3D). We verified that *Brn2*, *Braf*, and *Pten* were

236 correctly defloxed in the resulting melanomas (Supplementary Fig. 3E,F). In
237 summary, our data show that Brn2 acts as a tumor suppressor *in vivo.* As it has been
238 shown in humans and mice, induction of early proliferation induced by the presence
239 of the $BRAF^{V600E}$ mutation leads to senescence, but it can be bypassed when the
240 level of Pten is reduced [3,37,39,40]. It is important to note that in the absence of Pten in
241 the physiological context, proliferation of melanoblasts and melanocytes is not
242 induced as the reduction/lack of Pten promotes proliferation once the cells are
243 transformed [3,41]. On a Braf-Pten context the loss/reduction of Brn2 appears to induce
244 melanoma initiation after promoting proliferation and bypass/escape of senescence,
245 and then allows the tumor growth as was previously showed in vivo [3,37].
246
247 Reduction of BRN2 levels increases proliferation *in vivo* and *in vitro.*
248 The effect of *Brn2* loss on tumor growth prompted us to investigate whether *Brn2*
249 loss increases intra-tumor proliferation. Staining sections for Ki-67, a marker of
250 cycling cells, revealed that melanomas from Braf-Pten-Brn2-het/hom mice displayed
251 a significantly higher number of $Ki\text{-}67^{+}$ cells than Braf-Pten-Brn2-WT melanomas
252 (Figure 3A,B). To confirm this result, we injected Braf-Pten-Brn2 mice with
253 bromodeoxyuridine (BrdU) two hours prior to euthanization, to determine whether
254 melanoma cells were slow or fast-dividing. Braf-Pten-Brn2 melanomas had a
255 significantly higher number of $BrdU^{+}$ cells when Brn2 was heterozygous or
256 homozygous (Figure 3C,D). These results indicated that heterozygous loss of *Pten*
257 combined with heterozygous/homozygous loss of *Brn2* promotes melanoma
258 proliferation *in vivo*.

We next assessed whether Brn2 knockdown favors proliferation *in vitro* and whether this mechanism is conserved (i) between human and mouse and (ii) between transformed and non-transformed cells using Dauv-1 human melanoma cell line, and the Melan-a mouse melanocyte cell line. These cell lines express both Pten and Brn2 mRNA and protein (Supplementary Table 1). Dauv-1 cells carry a $BRAF^{V600E/+}$ mutation identical to that used in the mouse melanoma model system, and Melan-a cells are WT for Braf. siRNA-mediated knockdown of Brn2 significantly increased cell number 72 h after transfection of both cell lines (Figure 3E-G). Brn2 knockdown, assessed by western blot, led to an increase in cyclin D1 protein levels in both cell lines, but did not alter cyclin D1 mRNA levels, suggesting a regulation of cyclin D1 at the protein level (Figure 3F-H). Overall, the reduction of the Brn2 protein induces cell proliferation of the melanocytic lineage *in vivo* and *in vitro*.

Colony formation assays *in vitro* are classically used to show the importance of a gene in tumorigenesis, and indicate that a single cell may survive *in vitro* and proliferate to form a colony. Previous work has demonstrated that a reduction in Brn2 levels in melanoma cells has no effect on colony formation [42,43]. However, to test this in our model, mouse melanoma cell lines were established and characterized from the different independent Braf-Pten-Brn2 C57BL/6J mouse melanoma; the m50 and m6 cell lines were Brn2-WT, m59 and m36 were Brn2-het, and m82 and m8 were Brn2-hom (Supplementary Fig. 4A-F). The presence or absence of Brn2 did not decrease the ability of these melanoma cell lines to grow in syngeneic mice (Supplementary Table 2). In other words, it appears that the absence of Brn2 in these melanoma cells does not affect the implantation of the cells on the body wall, the proliferation after their transformation or the induction of angiogenesis in an

283 immunocompetent environment. We evaluated the capacity of the m50 (Brn2 WT),
284 m59 (het), and m82 (hom) cells to generate colonies and observed, in agreement
285 with previous observations obtained using BRN2 depletion, that the three cell lines
286 have similar abilities to form colonies (Supplementary Fig. 4G). Moreover, re-
287 expression of Brn2 using lentivirus infection in two independent m8 and m82 Braf-
288 Pten-Brn2-hom mouse melanoma cell lines, also indicated that BRN2 does not affect
289 their capacity to form colonies under these conditions (Supplementary Fig. 4H,I). In
290 conclusion, as shown in human cell lines, the number of colony forming units is
291 independent of the presence or absence of Brn2 and consequently this assay is
292 uninformative regarding the role of Brn2 in melanomagenesis.
293 We also evaluated the activity of $BRAF^{V600}$ (PLX4720), MEK (Binimetinib), and
294 PI3K (LY294002) inhibitors on the capacities of m50, m59 and m82 mouse
295 melanoma cell lines to form CFU and determined the IC50 of these drugs
296 (Supplementary Fig. 4J-O). Consistent with observations suggesting that BRN2 may
297 suppress cell death [43], Brn2-het/hom cells are more sensitive than WT cells to these
298 three drugs. We also evaluated the cooperativity of PLX4720 and LY294002 using
299 various concentrations of each drug, but we did not observe any cooperation/synergy
300 of these two drugs.
301
302 Mono-allelic loss of Brn2 induces melanoma metastasis.
303 We next evaluated the effects of Brn2 on metastasis formation *in vivo*. Since human
304 SKCM is known to spread to proximal lymph nodes (LNs), we assessed the presence
305 of pigmented cells in the inguinal LNs of tumor-bearing Braf-Pten-Brn2 mice.
306 Specifically, we estimated the volume of the various metastases present in LNs and

307 the number of pigmented areas after haematoxylin & eosin (HE) staining of LN
308 sections (Figure 4A-C). All Braf-Pten-Brn2 mice, irrespective of BRN2 status, showed
309 the presence of pigmented cells in both inguinal LNs. However, the LN volume of
310 Braf-Pten-Brn2-het mice was significantly higher than that of Braf-Pten-Brn2-WT and
311 Braf-Pten-Brn2-hom (Figure 4A,B). Similarly, Braf-Pten-Brn2-het LNs showed a
312 higher number of pigmented areas per mm^2 than Braf-Pten-Brn2-WT/hom mice
313 (Figure 4C).

314 To verify that the pigmented cells in the lymph nodes did not arise from cells in
315 which the Cre recombinase had not worked efficiently, we tested whether these
316 pigmented cells were properly defloxed for Brn2. The targeted Brn2-flox allele, used
317 in our mouse model, has an eGFP-cassette inserted downstream of the floxed *Brn2*
318 locus (Figure 4D). Thus the production of eGFP occurs once the upstream *Brn2* gene
319 is defloxed. Consistent with correct defloxing of *Brn2*, pigmented areas of LNs
320 expressed GFP in Braf-Pten-Brn2-het/hom mice, but not Braf-Pten-Brn2-WT mice
321 (Figure 4E). The pigmented cells present in Braf-Pten-Brn2-WT and Braf-Pten-Brn2-
322 het LNs also expressed Sox10, a melanocytic marker (Figure 4E), that co-localized
323 with eGFP-expression in Braf-Pten-Brn2-het mice confirming the melanocytic origin
324 of the pigmented cells observed.

325 To get a better understanding of melanomagenesis in the various Brn2-
326 WT/het/hom situations, we performed a transcriptomic analysis of the various Brn2
327 tumors and cell lines (Supplementary Data 3 and 4). The ontology enrichment
328 analysis indicated that the Braf-Pten-Brn2-het tumors were more inflamed than the
329 Braf-Pten-Brn2-WT tumors with increased neutrophil-associated gene expression
330 (Supplementary Fig. 5A). It also suggests that the extracellular-matrix was actively

remodeled and that these Braf-Pten-Brn2-het tumors were more subject to angiogenesis (Supplementary Fig. 5A). Pathway enrichment analysis supported these results as inflammatory gene expression signatures are enriched from both the WikiPathways and KEGG databases (Supplementary Fig. 5B,C). Significantly, the PI3K/AKT pathway was enriched in the Braf-Pten-Brn2-het tumors compared to the Braf-Pten-Brn2-WT in both WikiPathways and KEGG databases (Supplementary Fig. 5B,C), suggesting that AKT could be more phosphorylated in the Braf-Pten-Brn2-het tumors. This assumption was verified by Western-blot analysis where phosphorylation of AKT on S473, a surrogate of the AKT activity, and the phosphorylation of S6 on S235/236 were significantly increased in Braf-Pten-Brn2-het/hom tumors compared to Braf-Pten-Brn2-WT tumors (Supplementary Fig. 5D).

Gene Set Enrichment Analysis (GSEA) using the melanoma invasive signature from Verfaillie [44] indicated that Braf-Pten-Brn2-het tumors and cell lines were more invasive than Braf-Pten-Brn2-hom tumors and cell lines (Figure 4F). Moreover, from the GO, WikiPathways and KEGG 2019 analyses of the mouse melanoma tumors, the immune system (cytokine, neutrophil, macrophage) and angiogenesis are induced in Braf-Pten-Brn2-het tumors compared to Braf-Pten-Brn2-WT tumors (Supplementary Fig. 5A-C). This information suggests that Braf-Pten-Brn2-het cells have more potential to metastasize than Braf-Pten-Brn2-WT and Braf-Pten-Brn2-hom cells. In this respect, we tested the capacity of Braf-Pten-Brn2-hom (m82) mouse melanoma cell lines re-expressing or not Brn2 (m82 and m82+Brn2) to invade matrigel in 3D. In the presence of ectopic Brn2, the m82 Brn2 KO melanoma cell lines have more ability to invade (Figure 4G and S4I). Since AXL, a receptor tyrosine kinase (RTK), is associated with melanoma metastasis [45], we also evaluated

355 the level of Axl in mouse melanoma tumors and cells. Braf-Pten-Brn2-het cells
356 produce slightly more Axl mRNA than Brn2-WT/hom (Figure 4H). This upregulation
357 does not affect genes that are in *Cis* of Axl suggesting a specific regulation of Axl in a
358 Braf-Pten-Brn2-het context (Supplementary Fig. 5E-G). Moreover, when the levels of
359 both BRN2 and MITF are reduced in human melanoma cell lines, the level of AXL
360 mRNA is induced (Supplementary Fig. 6D,H,L,P,T). More precisely the level of AXL
361 is slightly, but significantly, higher in Gerlach and DAUV-1 cell lines in which the level
362 of AXL is already very high, and is higher in SK28 and 501Mel cell lines in which the
363 level of AXL is much lower than in Gerlach and DAUV-1 cell lines.
364 In conclusion, compared with Braf-Pten-Brn2-WT mice, melanoma initiation is
365 promoted in both Braf-Pten-Brn2-het/hom mice, but metastasis is promoted only in
366 Braf-Pten-Brn2-het mice. These observations are consistent with the fact that on a
367 Brn2-het/hom background melanoma initiation (proliferation and bypass/escape of
368 senescence) is induced and melanoma invasion and/or survival is inhibited on a
369 Brn2-hom background.
370
371 BRN2 binds to the *PTEN* promoter and BRN2 loss leads to the reduction of *PTEN*
372 transcription.
373 The PI3K-AKT pathway is induced in melanoma and its induction abrogates
374 $BRAF^{V600E}$-induced senescence [46,47]. The loss of *Pten*, a suppressor of the PI3K
375 pathway, induces melanoma initiation and proliferation *in vivo* [3,37]. Since our Braf-
376 Pten mouse melanoma model retained one functional allele of *Pten*, we hypothesized
377 that *Brn2* loss would induce less expression from the WT *Pten* allele, leading to the
378 increased PI3K-AKT signaling observed (Supplementary Fig. 5D) and consequent

melanoma initiation and proliferation. We therefore evaluated the number of Pten positive cells in the various Braf-Pten tumors by immunohistochemistry and found that Braf-Pten-Brn2-het/hom tumors showed fewer Pten-pos cells than Braf-Pten-Brn2-WT tumors (Figure 5A). This result was verified by western blotting of Braf-Pten tumor samples. The reduction of Brn2 correlates with the reduction of Pten in Braf-Pten-Brn2-het tumors compared to the Braf-Pten-Brn2-WT tumors (Figure 5B). In accordance with the reduced protein levels, the mRNA levels of Brn2 and Pten were significantly lower in Braf-Pten-Brn2-het/hom tumors than in Braf-Pten-Brn2-WT tumors, suggesting regulation of Pten at the transcriptional level (Figure 5C).

Next, we evaluated the mechanism of Pten repression mediated by reduced levels of Brn2 in the human Dauv-1, Gerlach, SK28, and 501Mel melanoma cell lines and in the non-transformed mouse Melan-a cell line. siRNA-mediated BRN2 knockdown led to significantly reduced PTEN protein and mRNA levels in cell lines having high BRN2 expression (Figure 5D,E and Supplementary Fig. 6). In cells with lower level of BRN2 (501Mel), the reduction of PTEN was not observed.

We examined the *PTEN* promoter for BRN2 binding sites conserved between humans and mice to determine whether BRN2 acts directly on *PTEN* and detected two potential Brn2 binding sites (BS1 and BS2) at the positions - 2,049 and +761 (numbering relative to TSS). Chromatin-immunoprecipitation (ChIP) for BRN2, performed on Dauv-1 melanoma cell extracts, followed by qPCR, revealed quantitative BRN2 binding to both binding sites, comparable to BRN2 binding on the PAX3 promoter (Figure 5F-H). IgG was used as a negative control.

To evaluate Pten promoter activity in response to BRN2, we cloned a 3.2-kb-human Pten promoter fragment containing the two BRN2 binding sites upstream the

luciferase gene to generate the hsPten::Luciferase reporter construct (Figure 5H). The analysis of human PTEN promoter activity showed an intrinsic activity of hsPten::Luciferase in human melanoma cells (Supplementary Fig. 7A,B). A consistent repression of PTEN transcription was observed when a smart-pool of siBRN2 was added. In contrast, PTEN transcription was activated following co-transfection of a BRN2 expression vector compared to empty vector in Dauv-1 and SK28 cell lines in luciferase assay (Figure 5I-L). We performed similar experiments with the mouse PTEN promoter, which was cloned upstream of the luciferase construct (Supplementary Fig. 7C-F); Brn2 activated Pten transcription in three mouse melanoma cell lines (m82, m59 and m50) (Figure 5M,N). In conclusion, BRN2 directly induces PTEN transcription.

MITF binds the *PTEN* locus and represses *PTEN* transcription.

The *MITF* gene encodes a key transcription factor that plays a major role in melanocyte and melanoma biology [18]. Several studies have reported that *MITF* transcription is directly repressed by BRN2 whereas a reduction in BRN2 levels leads to increased MITF levels [13,27,48], while another study showed that BRN2 induces MITF [49]. Likely both results are correct due to the versatile role of BRN2 as a transcription regulator whose activity may be dependent on context including genetic status and/or the environment [21,26,27].

Knowing the importance of MITF in the melanocyte lineage, we analyzed the consequences of modulation of MITF expression on PTEN. Using siRNA-mediated *MITF* knockdown in three human melanoma cell lines expressing high levels of MITF (501mel, SK28, HBL) led to a significant increase of PTEN protein and mRNA levels

(Figure 6A,B). In cells expressing lower levels of MITF, such as Gerlach and Dauv-1, we did not observe an increase of PTEN (Supplementary Fig. 6C,G). Next, to determine if MITF directly regulates PTEN expression through proximal enhancers we performed Cleavage Under Targets and Release Using Nuclease (CUT&RUN) with antibodies to MITF, as previously described,[50] and to H3K27Ac, revealing active chromatin, and against H3K4me3, revealing active and poised promoters, in SK28 cell lines that were wild type for *MITF* (MITF-WT) or had loss of function mutations in all alleles of it (ΔMITF) (Figure 6C) [50] . An MITF peak is present within the gene body of *PTEN* (intron 4), and a second one is 114kb downstream of the *PTEN* transcriptional start site (TSS) (i.e., +114kb). Both MITF peaks were centered on an M-box motif (5'-TCATGTG-3'). At both intron-4 and +114kb MITF peaks, the H3K27Ac signal was unchanged in ΔMITF mutant cell lines. However, six distal enhancers (painted light blue) exhibited a 2-fold greater H3K27ac signal in MITF mutant cell lines compared to wild-type cell lines (+140kb, +210kb, +230kb, +253kb, +301kb and +317kb), suggesting increased transcription of *PTEN* in the former. We confirmed the +140kb MITF peak after performing a quantitative ChIP experiments on 501Mel cells expressing MITF-HA (Figure 6D,E), using Tyrosinase (TYR) and PRM1 as positive and negative controls respectively. Overall, reduction of MITF results in an increase in PTEN mRNA expression. As such, it is plausible that Brn2 induces *Pten* transcription through two different, but concurrent mechanisms: (i) directly through BRN2 binding to the *PTEN* promoter to induce its transcription and (ii) indirectly via BRN2 modulating (repressing/inducing depending of the situation) MITF expression, with MITF binding to the 3' end of *PTEN* to inhibit its transcription. In the absence of BRN2, these mechanisms are disrupted and *PTEN* transcription is

451 downregulated in our conditions. In conclusion, MITF represses directly *PTEN*
452 transcription.

453 Overall, our results are consistent with a model in which reduction of BRN2
454 reduces PTEN transcription *in vitro* and *in vivo*, thus ramping up PI3K signaling and
455 inducing both the initiation of melanoma and the formation of metastases.

456

457 DISCUSSION

458 A well-established principle of cancer biology is that tumors are initiated by a
459 combination of oncogene activation together with loss of tumor suppressor
460 expression or activity. In melanoma, key oncogenic drivers, such as BRAF and
461 NRAS, have been well defined. Loss of P16 or PTEN tumor suppressor activity is
462 required to bypass oncogene-induced senescence and permit melanoma initiation.
463 However, while inactivation of tumor suppressors by mutation has been extensively
464 studied, it is less well understood how their activity may be modulated by changes in
465 their mRNA expression mediated by key melanoma-associated transcription factors.
466 At this point, it is important to note that factors involved in melanoma initiation will not
467 automatically reflect/translate into overall survival. Here, we identify BRN2, a key
468 transcription factor lying downstream of three melanoma-associated signaling
469 pathways (WNT/β-catenin, MAPK, and PI3K), as a tumor suppressor that functions
470 to regulate PTEN expression. Thus, monoallelic loss of *Brn2* promotes melanoma
471 initiation in a $Braf^{V600E}/Pten^{F/+}$ background where mono-allelic loss of *Pten* sensitizes
472 cells to loss of *Brn2*.

473 Previous work has primarily linked BRN2 to melanoma migration and invasion
474 *in vitro* and in xenograft experiments [13,20,42,51], but its role during melanoma initiation

and proliferation *in vivo* and in normal melanocytes had not been determined. We report that, consistent with *BRN2* playing a key role as a tumor suppressor in melanomagenesis, its locus is frequently lost in human skin cutaneous melanoma (SKCM) metastases, independently of their *NRAS* or *BRAF* status, and that *BRN2* status contributes to overall patient survival. Significantly, the overall survival of patients with a mono-allelic loss of PTEN is higher when the *BRN2* locus is intact.

Although these observations are consistent with BRN2 affecting human melanoma initiation and progression, loss of the *BRN2* locus is frequently associated with large segmental deletions that affect the long arm of chromosome 6 (6q) as it was observed in 14 out of 53, and 9 out of 32 out of primary melanoma and in 17 out of 21 melanoma cell lines [52-54], and confirmed in this study on a total of 205 out of 338 melanomas, and 11 out of 25 melanoma cell lines. It has already been shown that the loss of 6q was associated with a worse prognosis [52]. According to our observations, the loss of 6q is more detrimental for the overall survival than the focal loss of the *BRN2* locus (Fig. 1 and Fig. S1). Moreover, *in vitro* studies have shown that several genes are linked to melanomagenesis in the co-deleted region, including *ARID1B*, *CCNC*, and *ROS1*, although none have yet been shown to be functionally important in melanoma *in vivo* [48,55-61]. Similarly, we analysed the SKCM TCGA study to evaluate the overall survival comparing the mono allelic loss and the diploid state for *CCNC*, *ROS1* and *ARID1B* (Fig. S1). There is no statistical significance for *CCNC* ($p = 0.086$), *ROS1* ($p = 0.27$) or *ARID1B* ($p = 0.66$).

Thus, it might be argued that any of the genes located in this frequently deleted region may be acting to modulate melanoma initiation or progression. However, our functional mouse molecular genetics models show conclusively that

499 the heterozygous or homozygous loss of Brn2 promotes melanoma initiation and
500 initial growth. Similarly, our transcriptomic analysis showed that the mRNA levels of
501 the seven genes in the region co-deleted in humans (*Arid1b*, *Mchr2*, *Ccnc*, *Cdk19*,
502 *Dll1*, *Ros1*, and *Crybg1/Aim1*) were not affected in the mouse tumors (Braf-Pten-
503 Brn2-WT, Braf-Pten-Brn2-het and Braf-Pten-Brn2-hom). Collectively, these results
504 strongly suggest that the reduction/loss of Brn2 levels is a critical event that
505 cooperates with heterozygous Pten to promote the initiation and growth of
506 melanoma, independently of the co-deleted genes in melanoma. Finally, independent
507 initiation events are promoted when the level of Brn2 is lower than normal -
508 heterozygous or homozygous- since the number of independent melanoma is higher
509 in Braf-Pten-Brn2-het/hom mice than in Braf-Pten-Brn2-WT mice (Figure 2B). Our
510 observations are therefore consistent with BRN2 acting as a tumor suppressor in
511 melanoma, and are in full agreement with the predominantly mutually exclusive
512 pattern of BRN2 and Ki-67 *in situ* staining of invasive melanoma [20].

513 The presence of $Braf^{V600E}$ promotes proliferation prior to inducing senescence
514 and the loss of Pten results in senescence bypass [3,34,37]. As such, we believe that the
515 increased proliferation and tumor-initiation frequency observed in our
516 $Braf^{V600E}/Pten^{F/+}$ model arising as a consequence of the reduction of Brn2, is likely to
517 occur as a consequence of the ability of Brn2 to activate Pten expression and
518 suppress PI3K signaling either directly or potentially indirectly via Mitf repression
519 during early melanomagenesis. In other words, inactivation of Brn2 or a reduction in
520 its expression would lead to low expression of the remaining Pten allele and as a
521 consequence increase the probability of senescence bypass. This explanation fits
522 with the fact that in the absence of Pten on a $Braf^{V600E}$ background, the appearance

of the tumors is too rapid to observe any difference between Brn2 +/+, Brn2 F/+ or Brn2 F/F. According to our model the transcription regulation by Brn2 and Mitf would not affect the level of Pten since it is already lost. Moreover, in a context in which *Pten* is diploid (WT) and Brn2 is reduced (het or hom), the downregulation of Pten would be limited and not sufficient to act efficiently as a tumor-suppressor.

Although it might be argued that the increase in visible tumor number in a Braf-Pten-Brn2-het and -hom might be a consequence of the increased proliferation caused by reduction/loss of Brn2, as evidenced by the increased proportion of Ki-67 positive cells within tumours, we feel this is unlikely. For welfare reasons the Braf-Pten-Brn2-WT mice were euthanized with tumours (total volume 2 cm^3) after 4 weeks with about 8 tumours per mouse; by contrast the Braf-Pten-Brn2-het/hom mice were euthanized after 1.3 weeks with about 17 tumours per mouse of a similar size to the WT. Since tumour size is similar in the WT and Brn2 mutants, this indicates that the total number of cells in the WT and mutant tumours is similar and have undergone a similar number of cell divisions (though this occurred in a shorter time in the mutant). Since the WT and mutants have undergone a similar number of cell divisions, if proliferation were responsible for any increase in number of visible tumours then at 4 weeks the numbers of tumours in the WT should be the same as in the mutant at 1.3 weeks, whereas in fact, the tumour numbers in the WT were around 50% of those in the Brn2 mutants. Although we do not want to rule out a contribution of proliferation, the more likely explanation is that the reduction of BRN2 promotes the bypass of senescence (by reducing the level of Pten) or/and promotes survival of proliferating melanoma cells at the early stages of initiation.

Our *in vivo* data therefore reveal that melanocyte-specific Brn2 reduction in Braf-Pten mice promotes the initiation and progression of melanoma. Melanoma initiation is promoted after proliferation is induced through various proteins including Mitf and senescence bypassed in this case through reduction of the level of Pten. Melanoma progression is induced by promoting invasion when the level of Brn2 is intermediate after inducing Axl and modulating the immune system. In the future, we will have to evaluate the kinase activity of Axl in this context, and the consequences of its inhibition *in cellulo* and *in vivo* to understand the Mitf/Brn2/Axl *ménage à trois*. Altogether, we establish Brn2 as a central tumor suppressor, acting at different steps of melanomagenesis, and complement numerous other studies showing the effect of Brn2 on invasion [13-15,20,29,51].

Brn2 heterozygous mice were more prone to form LN metastases efficiently than mice that were *Brn2* WT when Pten was already heterozygous. The efficiency of the metastasis process depends on the status of *Brn2* as the number and size of each micro-metastasis was greater in Brn2 heterozygous than Brn2 wild-type melanoma. This is important as mono-allelic loss of *BRN2* in human, corresponding to *BRN2* heterozygous melanoma, occurs in 53% of human melanoma. In *Brn2* wild-type melanoma, the change of the level/activity of Brn2 is possible but the amount of protein found in Brn2 wild-type melanoma absorbs better transient Brn2 depletion than in *Brn2* heterozygous melanoma.

Some residual Brn2 activity might be required for efficient melanoma progression. On one hand, Braf-Pten-Brn2-het and Braf-Pten-Brn2-hom melanomas proliferate faster, and on the other hand, according to our results (Figure 4F,G) Braf-Pten-Brn2-hom melanomas have a reduced ability to invade compared to Braf-Pten-

570 Brn2-het melanomas. Moreover, the lack of BRN2 reduces migration and increases
571 the rate of apoptosis and/or anoikis [20,28,43]. In a more speculative way, one may think
572 that optimal melanoma progression may be associated with a series of proliferative
573 and invasive phases. In the absence of BRN2, cells are “fixed” in one stage and
574 cannot switch from “proliferative” to “invasive” states. These cells are mainly
575 proliferative and poorly invasive as we observed in Braf-Pten-Brn2-hom situation. In
576 the presence of Brn2 (as WT [two alleles] or heterozygous [one allele], the
577 corresponding mRNA and protein concentrations can be positively and negatively
578 modulated by external/internal factors. The modulation of the level of Brn2 is more
579 sensitive on a heterozygous background than on a WT background.

580 Altogether, one may understand that melanoma grows faster and forms
581 melanoma when Brn2 expression is not too high (proliferation handicap) but at the
582 same time not too low (migration/invasion/survival handicap). Indeed, on the one
583 hand, Brn2-het and Brn2-hom melanomas proliferate faster, and on the other hand,
584 Brn2-hom melanomas are handicapped to invade (Figure 4F,G), to migrate [20] and to
585 die by anoikis [28].

586 The formation of metastases is a multistep process in which cells proliferating
587 in the primary tumor, and surviving the metastatic process, must undergo a switch to
588 an invasive phenotype prior to a switch to a proliferative phenotype on site. Since the
589 switch from proliferation to invasion, and back, has been associated with the activity
590 of MITF, it is possible that for efficient metastatic colonization cells must be able to
591 modulate MITF expression via BRN2. In this respect, it is especially important to note
592 that BRN2 has been identified as a key regulator of MITF [13,49]. Consistent with the
593 observation that MITF and BRN2 are frequently observed in mutually exclusive

populations in melanoma, and that BRN2 may act *in vivo* as an MITF repressor [13], we have observed that in a non-tumoral context, the specific knock-out of Brn2 *in vivo* in melanocytes increases the level of Mitf (publication in preparation). Importantly, during progression of mouse Braf-Pten melanoma Mitf levels are modulated. During the initial phase of growth, melanoma cells are pigmented, indicative of Mitf activity, but later *in situ* they lose pigmentation and ability to produce Mitf ([62] and not shown). Although the reduction of Brn2 in Braf-Pten-Brn2 primary melanoma is not sufficient to re-induce Mitf mRNA and pigmentation in all cells of these primary melanomas, the Braf-Pten melanoma cells that formed LN metastases were pigmented and re-expressed Sox10, a key transcription activator of Mitf. Thus, during progression of Braf-Pten melanomas Mitf is produced during initial growth and subsequently repressed during the second phase, before being re-expressed in LN metastases. It seems therefore likely that one role of the residual BRN2 in the heterozygotes may be to facilitate the modulation of MITF expression during metastatic spread.

It has been shown that BRAF and PI3K induce BRN2 [15,16]. In consequence, it was expected that the level of BRN2 would decrease in the presence of such inhibitors. In addition, in the presence or absence of BRN2, melanoma cells are either more resistant or more sensitive to BRAF inhibitors, respectively [28,43]. This sensitivity would be associated with the function of BRN2 in DNA repair [43].

Although here we have focused on the role of BRN2 in melanoma, BRN2 is also expressed in a number of other cancer types including small cell lung cancer, neuroblastoma, glioblastoma and neuroendocrine prostate cancer [8-10]. While BRN2-mediated regulation of MITF is not likely to be important for non-melanoma cancers

618 that do not express MITF, the ability of BRN2 to modulate PTEN expression
619 uncovered here may play an equally important role in promoting the initiation and
620 progression of these cancer types. In this respect the inducible knockout mice
621 described here may represent an important tool to examine the role of BRN2 in non-
622 melanoma cancers.

623 In conclusion, our results identify Brn2 as a key tumor suppressor through its
624 ability to modulate Pten expression that, given the high prevalence of monoallelic
625 mutations, is likely to play a key role in initiation of human melanoma and likely other
626 BRN2-expressing cancer types. Since BRN2 expression is activated by PI3K
627 signaling via PAX3 [16], its ability to suppress PI3K signaling by increasing PTEN
628 expression may also provide cells with a negative feedback loop to control the PI3K
629 pathway. Moreover activation of BRN2 by MAPK signaling downstream BRAF [15] as
630 well as WNT/β-catenin signaling [14], may also permit coordination between these
631 pathways and the PTEN/PI3K axis. Finally, given the importance of BRN2 in
632 melanomagenesis identified here as well as its frequent heterozygosity, it may be
633 important to further explore whether tumors with low BRN2 expression may be more
634 susceptible to PI3K pathway inhibition, as it was shown for MAPK inhibitors. In this
635 respect, this mouse model of BRN2-deficient melanoma could be useful for the pre-
636 clinical testing of inhibitors for clinical development especially since it has been
637 shown that BRN2 is involved in DNA repair [43].
638

639 Figure legends

640

641 Figure 1. One *BRN2* allele is frequently lost in human melanoma and reduced BRN2
642 mRNA level correlates with reduced overall survival.
643 (A) Bar graph showing the status of the *BRN2* locus in human skin cutaneous
644 melanoma (SKCM) metastases (stage IV). Copy-number alterations (CNAs) were
645 estimated using the GISTIC algorithm. Two alleles (2a in black), one allele (1a in
646 red), no allele (0a in orange), and gain and/or amplification (G/Aa in blue) of the
647 *BRN2* locus are given.
648 (B) Pictogram showing the extent of segmental deletions (red or orange vertical lines)
649 that affect the *BRN2* locus on Chr.6q16 (dashed blue horizontal line) in SKCM
650 metastases.
651 (C) Kaplan-Meier curves comparing 10-year overall survival of SKCM patients diploid
652 for BRN2 (black line, n = 106) or those with mono-allelic (red n = 156). The TCGA
653 CNA-data set was analyzed (n = 309). Diploid *vs*. Mono-allelic loss: log-rank (Mantel-
654 cox) test (p = 0.067). Data were retrieved from TCGA on August 8, 2019.
655 (D) Kaplan Meier curves comparing melanoma patients with diploid status or mono-
656 allelic loss of *BRN2* in 118 regional metastatic melanoma patients (p = 0.003, log-
657 rank test) [31] and unpublished data.
658 (E) Kaplan-Meier curves comparing 30-year overall survival of SKCM patients to
659 BRN2 mRNA levels. Log-rank (Mantel-Cox) test (p = 0.03). Data were retrieved from
660 TCGA on August 8, 2019. Significance was defined as * ($p < 0.05$) and *** ($p \leq 0.001$).

661

662 Figure 2. Brn2 loss potentiates melanomagenesis in Braf-Pten mice.

663 (A) Macroscopic pictures of the dorsal view of mice with cutaneous melanomas
664 carrying mutations in the melanocyte lineage for Braf, Pten, and Brn2 after tamoxifen
665 induction at birth (p1, p2, and p3 – see Supplementary Fig. 3). *Tyr::CreER$^{T2/°}$;*
666 *Braf$^{V600E/+}$; Pten$^{+/+}$* (= Braf), *Pten$^{F/+}$* (= Pten), *Brn2$^{+/+}$* (=Brn2-WT), *Brn2$^{F/+}$* (= Brn2-het),
667 and *Brn2$^{F/F}$* (= Brn2-hom). Tumors are highlighted with arrows and the sizes of the
668 first growing tumors to appear are proportional to the diameters of the circles. F
669 means floxed allele.
670 (B) All Braf (n = 9), Braf-Brn2-het (n = 8), and Braf-Brn2-hom (n = 4) mice produced
671 cutaneous melanomas and their number was similar (1 to 2 tumors/mouse). All Braf-
672 Pten-Brn2-WT (n = 7), Braf-Pten-Brn2-het (n = 21), and Braf-Pten-Brn2-hom (n = 11)
673 mice produced cutaneous melanomas. Note that in the absence of Pten (*Pten$^{F/F}$*), the
674 appearance of the melanoma was too rapid to observe any difference between Brn2-
675 WT, Brn2-het, and Brn2-hom mice. Each dot corresponds to an individual mouse. As
676 control, mice of different genetic backgrounds were produced and not induced with
677 tamoxifen (Braf [n = 12], Braf-Brn2-het [n = 25], Braf-Brn2-hom [n = 11], Braf-Pten [n
678 = 7], Braf-Pten-Brn2-het [n = 13], and Braf-Pten-Brn2-hom [n = 6]; none of them
679 developed melanoma after 18 months, except one Braf-Pten-Brn2-het mouse that
680 developed one melanoma after 12 months. None of the mice that were wild-type for
681 *Braf* displayed any obvious phenotype, irrespective of the status of *Pten* or *Brn2,*
682 including melanomagenesis and hyperpigmentation.
683 (C) Growth rates of the first tumor appearing in each mouse for Braf-Brn2-WT, Braf-
684 Brn2-het, Braf-Brn2-hom, Braf-Pten-Brn2-WT, Braf-Pten-Brn2-het, and Braf-Pten-
685 het-Brn2-hom mice. The number of tumors is determined all along the life of the
686 mouse by checking the mice a minimum of twice a week. Statistical analysis was

687 performed using the two-tailed unpaired t-test. ns = non-significant, *p < 0.05, **p <
688 0.01, and *** p<0.001. Data are presented as mean values +/- SEM. Braf-Pten-Brn2-
689 het mice were euthanized in average 1.3 weeks after appearance of the first tumors
690 with an average of 16 tumors/mouse. Similar results were obtained with Braf-Pten-
691 Brn2-hom mice. Braf-Pten-Brn2-WT mice were euthanized at 4 weeks with an
692 average of 8 tumors even though they did not reach a total volume of $2cm^3$ except for
693 one mouse that was euthanized earlier (three weeks).
694
695 Figure 3. BRN2-het/hom induces proliferation *in vitro* and *in vivo.*
696 (A-D) Representative photomicrographs of Ki-67 (A) and BrdU (C) stainings of Braf-
697 Pten-Brn2-WT/het/hom tumors. $Ki\text{-}67^+$ cells are stained in red. Nuclei are stained in
698 blue. Scale bar = 40 µm. Three independent tumors for each genotype were used for
699 these experiments and three independent sections were used for each tumor. A 2-
700 way ANOVA with Dunnett's multiple comparisons tests were performed. Ki-67+ (B)
701 and BrdU (D) stainings of (A) and (C), respectively. Scale bar = 40 μm. Each dot
702 represents the result for one tumor.
703 (E) Growth rate is induced in Dauv-1 and Melan-a cell lines after reduction of Brn2
704 using siBRN2 and siScr as control (Scr = scramble). Three independent biological
705 and technical experiments were performed for each cell line and for each condition.
706 (F-H) Brn2 knock down induces Cyclin D1 protein but not its mRNA in melanocytes.
707 (F) Western blot analysis for Brn2, Cyclin D1, and actin after reduction of Brn2 in
708 Dauv-1 and Melan-a cells. Experiments were performed independently three times.
709 One representative western blot is shown (raw data are presented in Supplementary
710 Fig. 8). (G,H) Quantification of protein (G) and mRNA (H) levels for Dauv-1 cells after

siRNA-mediated knockdown (n = 3, independent experiments). For the proteins, all values were normalized against the background and corresponding actin loading control for each sample. Quantification was performed using *Image-J* software. For mRNA, all values were normalized against those of TBP. au = arbitrary units. Statistical analysis was performed using the two-tailed unpaired (B,D,E,H) and paired (G) t-tests. ns = non-significant, *$p < 0.05$, **$p < 0.01$, and ***$p < 0.001$. Data are presented as mean values +/- SEM.

Figure 4. Mono-allelic loss of *Brn2* induces melanoma metastasis.

(A) Upper panel: Representative photomicrographs of *in situ* inguinal lymph nodes (LN) of Braf-Pten-Brn2-WT/het/hom mice. Scale bar = 1 mm. The pigmented volume (mm^3) was estimated for each LN. Lower panel: Representative photomicrographs of haematoxylin & eosin (H&E) staining of LNs containing pigmented cells. Scale bar = 20 μm.

(B) Quantification of the pigmented volume of inguinal LNs in the upper panel of Figure (A). n = 3, 5, and 5 for WT, het, and hom.

(C) Quantification of the pigmented areas per mm^2 of inguinal LNs in the lower panel of Figure (A). Pigmented areas > 50 μm^2 were considered. n = 3, 5, and 3 for WT, het, and hom.

(D) Scheme showing the defloxing strategy of Brn2 in melanocytes of the primary tumor that releases eGFP expression upon the defloxing of *Brn2*.

(E) Representative photomicrographs, from four independent experiments, of serial LN sections of Braf-Pten-Brn2-WT and Braf-Pten-Brn2-het mice stained with H&E and the melanocyte marker Sox10. H&E staining was evaluated for one section and

GFP (green channel) and Sox10 staining (red channel) evaluated for an adjacent section. Scale bar = 20 μm.

(F) A melanoma invasive signature was significantly enriched in the Braf-Pten-Brn2-het tumors (left) and in the Braf-Pten-Brn2-het melanoma cell lines (right) compared to their Braf-Pten-Brn2-hom counterparts.

(G) Left: photomicrographs of m82 and m82-BRN2 mouse melanoma cells embedded as spheroids in 600 µg/mL matrigel at t0 (H0) and 18 hrs after (H18). Right : Boxes and plots represent the area of invasion (red lines on photomicrographs) quantified with *ImageJ* (n=54 for m82 cells and n=56 for m82-BRN2 cells). P-value<0.0001. au = arbitrary unit.

(H) Axl mRNA is significantly overexpressed in Braf-Pten-Brn2-het melanoma and melanoma cell lines (n = 10 and 2, respectively) compared to the Braf-Pten-Brn2-WT (n = 5 and 4, respectively) and Braf-Pten-Brn2-hom (n = 10 and 3, respectively) tumors.

Statistical analysis was performed using the two-tailed unpaired t-test for B, C, G and H (tumors) and an Anova test for H (cell lines). Data are presented as mean values +/- SEM for B and C, sd for H, and Box and whiskers (median, min to max) for G. ns = non-significant, *$p < 0.05$, ***$p < 0.001$, **** $p < 0.0001$.

Figure 5. Brn2 binds to the *Pten* promoter and Brn2 loss leads to Pten transcription reduction.

(A) Representative photomicrographs of immunohistochemistry staining of Pten (red) in Braf-Pten-Brn2-WT and Braf-Pten-Brn2 mouse melanomas are shown. Scale bar = 40 μm. Three independent tumors for each genotype were used for these

experiments and three independent sections were used for each tumor. A 2-way ANOVA with Dunnett's multiple comparisons tests were performed. The percentage of $Pten^{+}$ cells in WT and mutant tumors is shown.

(B) Western blot analysis of Brn2, Pten and actin for Braf-Pten-WT and Braf-Pten-Brn2 from at least three tumors of each genotype. One representative example is presented, raw data are presented in Supplementary Fig. 8. The relative intensities of the band were estimated with *ImageJ*.

(C) RT-qPCR of Brn2 and Pten from Braf-Pten-WT and Braf-Pten-Brn2 melanomas. Three independent mouse melanomas per genotype were analyzed. Data were normalized against the values of Gapdh. au = arbitrary unit.

(D) Western blot analysis of BRN2, PTEN and ACTIN from Dauv-1 human melanoma cells and Melan-a mouse melanocytes after siRNA mediated knockdown. A representative western blot is shown, raw data are presented in Supplementary Fig. 8. Scr = Scramble.

(E) RT-qPCR of BRN2 and PTEN from human melanoma cells (Dauv-1) and mouse melanocytes (Melan-a) after siRNA-mediated knockdown. Specific primers were used for human and mouse samples. Dauv-1 (n = 6), Melan-a (n = 4), independent experiments. Data were normalized against the values for TBP (Dauv-1) or Gapdh (Melan-a).

(F) ChIP assays of BRN2 binding to the *PTEN* promoter in Dauv-1 melanoma cells. All data shown are representative of at least three independent assays.

(G) Quantification of the ChIP-qPCR, plotted and normalized against IgG as the reference. au = arbitrary unit. n=6, 3, 4 and 3 for BRN2 CDS, PAX3 prom, BS1 and BS2, respectively.

(H) Scheme of the human *PTEN* promoter containing two BRN2 binding sites (BS) represented as colored circles. Note that BS are conserved between humans and mice. TSS = transcription start site. Exons (X) 1 and 2 are shown as horizontal rectangles. The translation start site (ATG) and the end of exon 1 are indicated. All numbering is relative to the TSS (+1). Representation of the reporter luciferase (luc) construct with or without *PTEN* promoter.

(I-N) Human and mouse *PTEN* promoter activities were evaluated in human Dauv-1 (I,K), SK28 (J,L), and in mouse m82 [Brn2-hom], m59 [Brn2-het], and m50 [Brn2-WT] (M,N) melanoma cell lines either in the presence of siScr (scramble) or siBrn2 (smart-pool) (I,J,M) or in the presence of expression vector of BRN2 (CMV::BRN2) (L,N). The experiments were independently performed four (I,J,K) and three (L) times. They were performed three independent times for m82 and m50, seven for m59 (M), and seven times for m82, six for m59 and four for m50 (N).

Statistical analysis was performed using the two-tailed unpaired t-test for C, E, G and paired t-test for I-N. Data are presented as mean values +/- SEM for C, E, G, I-M. Box and whiskers (median, min to max) for N. ns = non-significant, *$p < 0.05$, ***$p < 0.001$, and ****$p < 0.0001$.

Figure 6. MITF binds downstream of *PTEN* gene, MITF loss induces its transcription, and enhancers flanking *PTEN* are activated in MITF-depleted cells.

(A) Western blot analysis of MITF and PTEN from human melanoma cells (501mel, SK28, and HBL) after siRNA-mediated knockdown. Actin was used as a loading control. A representative western blot out of three is shown, raw data are presented in Supplementary Fig. 8. The molecular weight is indicated in kDa. Scr = Scrambled.

807 (B) RT-qPCR of MITF and PTEN from human melanoma cells (501mel and SK28)
808 after siRNA-MITF and Scr knockdown. All values were normalized against TBP. The
809 analysis was performed on three independent experiments with technical triplicates,
810 au = arbitrary unit.
811 (C) Screenshot of IGV genome browser (GRCH37/hg19) visualization of MITF,
812 H3K27Ac and H3K4me3 binding to the *PTEN* locus in SkMel28 cell lines that are
813 MITF-WT or mutant (i.e., MITF-ΔX6 = ΔMITF). Blue boxes below MITF and
814 H3K27Ac tracks: signal above IgG background (i.e., peaks) called by MACS2. PTEN
815 and downstream regions are shown, blue arrows indicate strand orientation and
816 horizontal rectangles the exons. Y-axes are scaled per antibody sample. Anti-MITF
817 CUT&RUN peaks present in WT cells that harbor an M-Box binding motif are painted
818 grey. Six distal enhancers (painted light blue) exhibited a 2-fold greater H3K27ac
819 signal in MITF mutant cell lines compared to wild-type cell lines. At least two
820 CUT&RUN biological replicates were performed for MITF, H3K27ac and H3K4me3.
821 (D) ChIP assays of MITF binding downstream of *PTEN* in 501mel human melanoma
822 cells stably expressing HA-Tagged MITF (location +140kb). ChIP assays are
823 performed using an antibody against HA and analyzed after a 30-cycle PCR
824 (exponential phase). The tyrosinase promoter (*TYR*) and *PRM1* were used as
825 positive and negative controls, respectively. Input represents approximately 3% of
826 the input used for the ChIP assay. H3 (histone H3) and IgG (Immunoglobulin G) were
827 used as positive and negative technical controls for each region of interest,
828 respectively. The oligonucleotides, their positions on the genome, and sizes of the
829 amplified fragments are shown in Supplementary Tables 3 and 4. All data shown are

representative of three independent assays. * corresponds to the remaining oligonucleotides.

(E) Quantification of the ChIP–qPCR presented in (D) is plotted and normalized against IgG as a reference. au = arbitrary unit. PRM1 (-): PRM1 (negative control), TYR (+): tyrosinase promoter (positive control).

Statistical analysis was performed using the two-tailed unpaired t-test.

Data are presented as mean values +/- SD. ns = non-significant, *$p < 0.05$, **$p < 0.01$, and ***$p < 0.001$.

METHODS

Detailed materials and methods are given in the supplemental information.

TCGA data

All TCGA data for somatic mutations, copy number alterations (CNAs), RNA-seq gene expression, and clinical data for skin cutaneous melanoma were retrieved from the National Cancer Institute (NCI) Genomic Data Commons (GDC) thorough its GDC Application Programming Interface (API) using the TCGAbiolinks package or the CGDS-R package to query the Cancer Genomic Data Server (CGDS) from cBioPortal.

Copy number analysis (CNA)

Preprocessed copy number data was obtained from cBioportal. Copy number data sets generated by the GISTIC 2.0 algorithms, specifically the allthresholded.bygenes.txt of the GISTIC output were used. Samples with GISTIC copy-number values of “-1” were considered as mono-allelic loss (red) and samples with GISTIC copy-number values of “-2” as bi-allelic loss (orange). TCGA dataset CNA-data set (n = 367). BRN2 CNA classified as gain/amplification (GISTIC > “+1” or “+2”) are not shown (n = 29, 7.9%).

Level of expression of BRN2 mRNA in melanoma patients

BRN2 mRNA levels were obtained from RNA sequencing data analyzed using the RNA Seq V2 RSEM pipeline as transcripts per million reads (TPM).

Mouse Models

Mice were bred and maintained in the specific pathogen-free mouse colony of the Institut Curie, in accordance with the institute's regulations and French and European Union laws. Experimental procedures were specifically approved by the ethics committee of the Institut Curie CEEA-IC #118 (CEEA-IC 2016-001) in compliance with the international guidelines. The transgenic *Tyr::Cre*$^{ERt2\text{-}Lar}$ *(also called Tyr::Cre*^{ERt2}*), Braf*$^{V600E/+}$, *Pten*, and *Brn2* mice have been described, characterized, and backcrossed onto a C57BL/6 background for more than ten generations [33-35,38,63]. Genotyping were performed accordingly (Supplementary Tables 3 and 4).

In vivo *gene activation/deletion and melanoma monitoring*

Newborn mice were treated dorsally with 0.4 µg/day/ouse tamoxifen from P1 to P3. Non-tamoxifen-induced mice of the same genotype were used as controls. Developing skin excrescences > 3 mm diameter were considered to be melanomas, and validated after growth. Mice were checked two-three times a week to estimate the volume of the tumors. They were euthanized and autopsied four weeks after tumor appearance or once the tumors reached 2 cm^3. Mouse melanomas were excised, rinsed in cold PBS snap-frozen in liquid nitrogen for subsequent transcriptomic and western blot analysis and fixed in 4% PFA and embedded in paraffin or OCT for histological analysis and immunostaining.

Immunohistochemistry of mouse melanoma and inguinal lymph nodes

Paraffin-embedded mouse melanomas were sectioned into 7-µm-thick transverse sections and stained with hematoxylin/eosin (H&E), as previously described [64].

887 Antibodies are from Nova-Costra for Ki-67, BD Biosciences for BrdU, from Abcam for
888 SOX10 and Cell signaling for PTEN. Images were captured using a ZEISS Axio
889 Imager 2 with Axiocam 506 color cameras. Image analysis was performed using
890 ZEISS ZEN, Adobe Photoshop, and *ImageJ* software. Quantifications of Ki-67 and
891 BrdU stainings were determined as a percentage. The percentage of Ki-67^{+} and
892 BrdU^{+} cells from three fields (1,000-2,000 cells/field) from three independent tumors
893 per genotype was determined and normalized.
894
895 *Protein extraction from tumors*
896 All steps were performed at 4°C. Tissues were transferred to a tube containing 2.8-
897 mm stainless steel beads and 1mL RIPA buffer supplemented with sodium
898 orthovanadate prior adding complete protease inhibitor and PhosSTOP (Roche).
899 Tissues were homogenized followed by centrifugation at 17,949 g for 1 min.
900 Supernatants were transferred and centrifuged for 20 min at 15,294 g. Supernatants
901 were collected and incubated with 200μL previously PBS-washed G-Sepharose
902 beads for 2h. Samples were centrifuged at 15,294 g for 5 min and quantified using
903 the Bradford assay.
904
905 *Microarray analysis*
906 Only one tumor per mouse was considered and corresponding to the biggest one.
907 Tumors had the same size since we harvested tumors for transcriptomic analyses
908 when they reached a size of 1cm^3. RNA from mouse melanomas (5 Braf-Pten-Brn2-
909 WT, 10 Braf-Pten-Brn2-het, and 10 Braf-Pten-Brn2-hom) and mouse melanoma cell
910 lines (4 Braf-Pten-Brn2-WT, 2 Braf-Pten-Brn2-het, and 3 Braf-Pten-Brn2-hom)

established from the mouse melanoma tumors was extracted using the miRNeasy Kit (Qiagen, #217004). Complete protocol can be found in the supplementary information.

In brief, 11µg cRNA hybridized to mouse MOE430 gene expression Affymetrix microarrays (Affymetrix, #900443). The microarray data were normalized using the RMA (Robust Multichip Average) function of the edgeR package [65]. Differentially expressed gene analysis was performed with R, for the cell lines and the tumors using the limma package [66] available from Bioconductor (http://www.bioconductor.org). An enriched gene-ontology (Gene-Ontology Biological-Process, 2018) and pathway (WikiPathways human, 2019 & KEGG human, 2019) analysis was performed on the 296 genes found overexpressed in the Braf-Pten-Brn2-het compared to the Braf-Pten-Brn2-WT using Enrichr [67]. Gene-set enrichment analysis (GSEA) was performed using the "Verfaillie" signature [44].

Cell lines

Melan-a and C57BL/6 9v cells were grown as previously described [4,68]. 501mel, 501mel-MITF-HA, HBL, SK-Mel-28 (SK28), Gerlach and Dauv-1 cells were grown in RPMI 1640 media supplemented with 10% FCS and 1% Penicillin-Streptomycin [69-71]. SK28Δex6 melanoma cells lacking Mitf was previously produced [50]. Cells are routinely tested for the absence of mycoplasmas using MycoAlert (Lonza). The origin and the main genetic characteristics of the cell lines are given in the supplemental information. Mouse melanoma cell lines were established as previously described [72].

Genomic DNA extraction and genotyping from cell culture

Genomic DNA was extracted from melanoma cell lines and column-purified with the QIAamp Kit (QIAGEN). See Supplementary Tables 3 and 4.

siRNA-mediated knock-down

siRNA targeting human BRN2 and MITF was purchased from Dharmacon as a SMART-pool mix of four sequences. siRNA targeting PTEN from Santa Cruz Biotech. Si Scramble (siSCR), with no known human or mouse targets, was purchased from Eurofins Genomics (Supplementary Table 5). Briefly, cells were transfected with Lipofectamine 2000 with 25-200 pmol siRNA or siSCR (according to the types of experiments) and assayed for mRNA expression, protein content or luciferase activity 48 or 72 h post-transfection.

Clonogenic assays

For clonogenic assays, six-well tissue culture plates were seeded with 500 cells in complete medium. The medium was changed 24 h after cell seeding and replaced with complete medium containing the indicated concentrations of Binimetinib (Selleck), MK-2206 2HCl (Selleck), LY294002 (Calbiochem) or PLX4720 (Axon Medchem). After 9 days of incubation, colonies were fixed with 4% PFA (paraformaldehyde), stained with Crystal violet in 10% ethanol, and counted on images. IC50 were determined for each pharmacological agent and for each cell line using the number of colonies in mock treated condition as the top response. Cell lines have been treated with Binimetinib from 10^{-3} to 100 μM, with PLX4720 from 10^{-3} to 100 μM, with LY294002 from 5.10^{-3} to 50 μM and with MK-2206 from 10^{-3} to 10 μM. We used the resulted sigmoidal curves to calculate the IC50 with Graphpad Prism. Experiments were performed at least in triplicate.

960

961 *Western blotting and detection*

962 Whole-cell lysate was prepared from cell lines using RIPA buffer supplemented with
963 sodium orthovanadate, complete inhibitor, and PhosSTOP. SDS-PAGE was carried
964 out on 10% polyacrylamide protein gels. Following the transfer of the proteins, the
965 nitrocellulose membranes were blocked in TBST with 5% non-fat dry milk for 1.5h at
966 RT and then probed with various antibodies. BRN2, Cyclin D1, PTEN, phospho-S6,
967 S6, phospho-AKT, and AKT antibodies were from Cell signaling, MITF from Abcam,
968 β-actin and vinculin from Sigma. Secondary antibodies were either HRP-conjugated
969 goat anti-rabbit or anti-mouse IgG. Blots were incubated in ECL (Pierce) and
970 revealed using ECL hyperfilm (GE Healthcare). All primary antibodies were used at a
971 dilution of 1/1,000, except β-actin and vinculin (1/5,000). All secondary antibodies
972 were used at a dilution of 1/20,000. Quantification of the western blots was
973 performed using *ImageJ* software. See table key ressources

974

975 *Chromatin immunoprecipitation*

976 ChIP experiments were performed as previously described [4], and see Supplementary
977 Table 6. ChIP assays of BRN2 binding to the *PTEN* promoter. ChIP assays were
978 performed using an antibody against BRN2 and analyzed after 30-cycle PCR in
979 exponentially growing phase of Dauv-1 melanoma cells. *PAX3* promoter (prom.) and
980 Brn2 coding sequences (CDS) were used as positive and negative controls,
981 respectively. Input represents approximately 0.4% of the input used for the ChIP
982 assay. H3 (histone H3) and IgG (Immunoglobulin G) were used as positive and
983 negative controls for each region of interest, respectively. The oligonucleotides, their

position on the genome, and the sizes of the amplified fragments are given in Supplementary Tables 3 and 4.

RNA extraction and (ChIP) RT-qPCR

Tissues were crushed with a mortar and pestle, and stainless steel beads. Qiazol was used to homogenize the samples prior extracting RNA using the miRNeasy Kit. Purified RNA was reversed transcribed using M-MLV Reverse Transcriptase. Real-time quantitative PCR (qPCR) was performed using iTaq™ Universal SYBR Green Supermix. Each sample was run in technical triplicates and the quantified RNA normalized against TBP (human) or Gapdh (mouse) as housekeeping transcripts (Supplementary Tables 3 and 4).

Software

GraphPad PRISM, R version 3.6.3 (R Foundation for Statistical Computing, Vienna, Austria), Adobe Illustrator, Adobe Photoshop, and Microsoft Power Point software were used to analyze data and generate all graphs and figures.

Quantification and statistical analysis

Cell culture-based experiments were performed in at least biological triplicate and validated three times as technical triplicates. P-values for the comparison of two groups were calculated using the unpaired Student t-test or Mann-Whitney test. P-values for the comparison of multiple groups were calculated using the analysis of variance (ANOVA) and Fisher's least significant difference tests. P-values for categorical data were calculated using the Chi-square test. P-values for the

comparison of Kaplan–Meier curves were calculated using the log-rank (Mantel–Cox) or Gehan-Breslow-Wilcoxon test giving weight to the early events. P-values were reported as computed by Prism 6.

Data availability

Microarray gene expression data that support the findings of this study have been deposited in Gene Expression Omnibus (GEO) with the accession codes GSE126524 (https://www.ncbi.nlm.nih.gov/geo/query/acc.cgi?acc=GSE126524) and GSE163085 (https://www.ncbi.nlm.nih.gov/geo/query/acc.cgi?acc=GSE163085). The TCGA Skin Cutaneous Melanoma data referenced during the study are available in a public repository from the National Cancer Institute (NCI) Genomic Data Commons (GDC) website (https://portal.gdc.cancer.gov). Cut&Run assay data that support the findings of this study have been deposited in Gene Expression Omnibus (GEO) with the accession codes GSE153020 (https://www.ncbi.nlm.nih.gov/geo/query/acc.cgi?acc=GSE153020). All the other data supporting the findings of this study are available within the article and its supplementary information files and from the corresponding author upon reasonable request. A reporting summary for this article is available as a Supplementary Information file. The data that support the findings of this study are available from the corresponding author upon reasonable request.

Acknowledgements

We are grateful to Dorothy C Bennett, Ghanem Ghanem, Florence Faure, and Meenhard Herlyn for providing cell lines. Hong Wu for providing Pten flox mice. We thank the Institut Curie staff responsible for the animal colony (especially P. Dubreuil), and the histology (S.

Lebouchet), FACS (C. Lasgi), and PICT-IBiSA imaging (C. Lovo) facilities. This work was supported by the Ligue nationale contre le cancer, INCa, ITMO Cancer, Fondation ARC (PGA), and is under the program «Investissements d'Avenir» launched by the French Government and implemented by ANR Labex CelTisPhyBio (ANR-11-LBX-0038 and ANR-10-IDEX-0001-02 PSL). MH had a fellowship from PSL and FRM, PS had a fellowship from INSERM, and MLC had a fellowship from FRM. CRG was supported by the Ludwig Institute for Cancer Research. RC was supported in part by a grant from the National Institutes of Health (AR062547, RAC) and a postdoctoral fellowship from the American Association for Anatomy (CK). ES was supported from the Research Fund of Iceland (184861-053). LL and ES are supported by a Jules Verne grant.

Author contributions

M.H., P.S., V.P., J.R., V.D., M.L.C., C.P.K., M.P., F.R., N.C., A.S., L.S.C., L.M., M.L., and G.B.J. conducted the experiments

M.H., P.S., R.A.C, C.R.G. and L.L. designed the experiments

M.H., P.S., V.P., F.G., V.D., Z.A., A.S., A.B., I.D., C.R.G., and L.L. wrote and reviewed the manuscript

C.R.G., and L.L. secured the funding

D.M. and E.S. provided reagents

I.D., A.S., C.R.G. provided expertise and feedback

Declaration of Interests

The authors declare no competing interests.

Ethical rules

Animal care, use, and experimental procedures were conducted in accordance with recommendations of the European Community (86/609/EEC) and Union (2010/63/UE) and

the French National Committee (87/848). Animal care and use were approved by the ethics committee of the Curie Institute in compliance with the institutional guidelines.

References

1. Davies, H. *et al.* Mutations of the BRAF gene in human cancer. *Nature* 417, 949-54 (2002).
2. Eskandarpour, M. *et al.* Frequency of UV-inducible NRAS mutations in melanomas of patients with germline CDKN2A mutations. *J Natl Cancer Inst* 95, 790-8 (2003).
3. Conde-Perez, A. *et al.* A caveolin-dependent and PI3K/AKT-independent role of PTEN in beta-catenin transcriptional activity. *Nat Commun* 6, 8093 (2015).
4. Delmas, V. *et al.* Beta-catenin induces immortalization of melanocytes by suppressing p16INK4a expression and cooperates with N-Ras in melanoma development. *Genes & Development* 21, 2923-35 (2007).
5. Bennett, D.C. Genetics of melanoma progression: the rise and fall of cell senescence. *Pigment Cell Melanoma Res* 29, 122-40 (2016).
6. Gray-Schopfer, V.C. *et al.* Cellular senescence in naevi and immortalisation in melanoma: a role for p16? *Br J Cancer* 95, 496-505 (2006).
7. Gembarska, A. *et al.* MDM4 is a key therapeutic target in cutaneous melanoma. *Nature medicine* 18, 1239-47 (2012).
8. Schreiber, E. *et al.* Astrocytes and glioblastoma cells express novel octamer-DNA binding proteins distinct from the ubiquitous Oct-1 and B cell type Oct-2 proteins. *Nucleic Acids Res* 18, 5495-503 (1990).
9. Bishop, J.L. *et al.* The Master Neural Transcription Factor BRN2 Is an Androgen Receptor-Suppressed Driver of Neuroendocrine Differentiation in Prostate Cancer. *Cancer Discov* 7, 54-71 (2017).
10. Ishii, J. *et al.* POU domain transcription factor BRN2 is crucial for expression of ASCL1, ND1 and neuroendocrine marker molecules and cell growth in small cell lung cancer. *Pathol Int* 63, 158-68 (2013).
11. Chitsazan, A. *et al.* Unexpected High Levels of BRN2/POU3F2 Expression in Human Dermal Melanocytic Nevi. *J Invest Dermatol* 140, 1299-1302 e4 (2020).
12. Colombo, S., Champeval, D., Rambow, F. & Larue, L. Transcriptomic analysis of mouse embryonic skin cells reveals previously unreported genes expressed in melanoblasts. *The Journal of investigative dermatology* 132, 170-8 (2012).
13. Goodall, J. *et al.* Brn-2 represses microphthalmia-associated transcription factor expression and marks a distinct subpopulation of microphthalmia-associated transcription factor-negative melanoma cells. *Cancer Res* 68, 7788-94 (2008).
14. Goodall, J. *et al.* Brn-2 expression controls melanoma proliferation and is directly regulated by beta-catenin. *Mol Cell Biol* 24, 2915-22 (2004).
15. Goodall, J. *et al.* The Brn-2 transcription factor links activated BRAF to melanoma proliferation. *Mol Cell Biol* 24, 2923-31 (2004).
16. Bonvin, E., Falletta, P., Shaw, H., Delmas, V. & Goding, C.R. A phosphatidylinositol 3-kinase-Pax3 axis regulates Brn-2 expression in melanoma. *Mol Cell Biol* 32, 4674-83 (2012).

17. Cook, A.L., Smith, A.G., Smit, D.J., Leonard, J.H. & Sturm, R.A. Co-expression of SOX9 and SOX10 during melanocytic differentiation in vitro. *Exp Cell Res* 308, 222-35 (2005).
18. Goding, C.R. & Arnheiter, H. MITF-the first 25 years. *Genes Dev* (2019).
19. Boyle, G.M. *et al.* Melanoma cell invasiveness is regulated by miR-211 suppression of the BRN2 transcription factor. *Pigment cell & melanoma research* 24, 525-537 (2011).
20. Zeng, H. *et al.* Bi-allelic Loss of CDKN2A Initiates Melanoma Invasion via BRN2 Activation. *Cancer Cell* 34, 56-68 e9 (2018).
21. Smith, M.P. *et al.* A PAX3/BRN2 rheostat controls the dynamics of BRAF mediated MITF regulation in MITF(high) /AXL(low) melanoma. *Pigment Cell Melanoma Res* (2018).
22. Potterf, S.B., Furumura, M., Dunn, K.J., Arnheiter, H. & Pavan, W.J. Transcription factor hierarchy in Waardenburg syndrome: regulation of MITF expression by SOX10 and PAX3. *Hum Genet* 107, 1-6 (2000).
23. Bondurand, N. *et al.* Interaction among SOX10, PAX3 and MITF, three genes altered in Waardenburg syndrome. *Hum Mol Genet* 9, 1907-17 (2000).
24. Vivas-Garcia, Y. *et al.* Lineage-Restricted Regulation of SCD and Fatty Acid Saturation by MITF Controls Melanoma Phenotypic Plasticity *Molecular Cell* 77, 120-139 (2020).
25. Simmons, J.L., Neuendorf, H.M. & Boyle, G.M. BRN2 and MITF together impact AXL expression in melanoma. *Experimental Dermatology* doi: 10.1111/exd.14225(2020).
26. Fane, M.E., Chhabra, Y., Smith, A.G. & Sturm, R.A. BRN2, a POUerful driver of melanoma phenotype switching and metastasis. *Pigment Cell Melanoma Res* 32, 9-24 (2019).
27. Berlin, I. *et al.* Phosphorylation of BRN2 modulates its interaction with the Pax3 promoter to control melanocyte migration and proliferation. *Molecular and cellular biology* 32, 1237-47 (2012).
28. Pierce, C.J. *et al.* BRN2 expression increases anoikis resistance in melanoma. *Oncogenesis* 9, 64 (2020).
29. Pinner, S. *et al.* Intravital imaging reveals transient changes in pigment production and Brn2 expression during metastatic melanoma dissemination. *Cancer Research* 69, 7969-77 (2009).
30. Arozarena, I. *et al.* In melanoma, beta-catenin is a suppressor of invasion. *Oncogene* 30, 4531-43 (2011).
31. Cirenajwis, H. *et al.* NF1-mutated melanoma tumors harbor distinct clinical and biological characteristics. *Mol Oncol* 11, 438-451 (2017).
32. Shain, A.H. *et al.* Genomic and transcriptomic analysis reveals incremental disruption of key signaling pathways during melanoma evolution *Cancer Cell* 34, 45-55 (2018).
33. Yajima, I. *et al.* Spatiotemporal gene control by the Cre-ERT2 system in melanocytes. *Genesis* 44, 34-43 (2006).
34. Dhomen, N. *et al.* Oncogenic Braf induces melanocyte senescence and melanoma in mice. *Cancer Cell* 15, 294-303 (2009).
35. Lesche, R. *et al.* Cre/loxP-mediated inactivation of the murine Pten tumor suppressor gene. *Genesis* 32, 148-9 (2002).

36. Dhomen, N. *et al.* Inducible expression of (V600E) Braf using tyrosinase-driven Cre recombinase results in embryonic lethality. *Pigment Cell Melanoma Res* 23, 112-20 (2010).
37. Dankort, D. *et al.* Braf(V600E) cooperates with Pten loss to induce metastatic melanoma. *Nat Genet* 41, 544-52 (2009).
38. Jaegle, M. *et al.* The POU proteins Brn-2 and Oct-6 share important functions in Schwann cell development. *Genes Dev* 17, 1380-91 (2003).
39. Bennett, D.C. Human melanocyte senescence and melanoma susceptibility genes. *Oncogene* 22, 3063-9 (2003).
40. Michaloglou, C. *et al.* BRAFE600-associated senescence-like cell cycle arrest of human naevi. *Nature* 436, 720-4 (2005).
41. Puig, I. *et al.* Deletion of Pten in the mouse enteric nervous system induces ganglioneuromatosis and mimics intestinal pseudoobstruction. *J Clin Invest* 119, 3586-96 (2009).
42. Simmons, J.L., Pierce, C.J., Al-Ejeh, F. & Boyle, G.M. MITF and BRN2 contribute to metastatic growth after dissemination of melanoma. *Sci Rep* 7, 10909 (2017).
43. Herbert, K. *et al.* BRN2 suppresses apoptosis, reprograms DNA damage repair, and is associated with a high somatic mutation burden in melanoma. *Genes Dev* 33, 310-332 (2019).
44. Verfaillie, A. *et al.* Decoding the regulatory landscape of melanoma reveals TEADS as regulators of the invasive cell state. *Nature communications* 6, 6683 (2015).
45. Muller, J. *et al.* Low MITF/AXL ratio predicts early resistance to multiple targeted drugs in melanoma. *Nat Commun* 5, 5712 (2014).
46. Davies, M.A. *et al.* Integrated Molecular and Clinical Analysis of AKT Activation in Metastatic Melanoma. *Clin Cancer Res* 15, 7538-7546 (2009).
47. Vredeveld, L.C. *et al.* Abrogation of BRAFV600E-induced senescence by PI3K pathway activation contributes to melanomagenesis. *Genes Dev* 26, 1055-69 (2012).
48. Thurber, A.E. *et al.* Inverse expression states of the BRN2 and MITF transcription factors in melanoma spheres and tumour xenografts regulate the NOTCH pathway. *Oncogene* 30, 3036-48 (2011).
49. Wellbrock, C. *et al.* Oncogenic BRAF regulates melanoma proliferation through the lineage specific factor MITF. *PLoS ONE* 3, e2734 (2008).
50. Dilshat, R. *et al.* MITF reprograms the extracellular matrix and focal adhesion in melanoma. *Elife*, 10:e63093 (2021).
51. Thomson, J.A. *et al.* The Brn-2 gene regulates the melanocytic phenotype and tumorigenic potential of human melanoma cells. *Oncogene* 11, 691-700 (1995).
52. Healy, E. *et al.* Prognostic significance of allelic losses in primary melanoma. *Oncogene* 16, 2213-8 (1998).
53. Bastian, B.C., LeBoit, P.E., Hamm, H., Brocker, E.B. & Pinkel, D. Chromosomal gains and losses in primary cutaneous melanomas detected by comparative genomic hybridization. *Cancer Res* 58, 2170-5 (1998).
54. Guan, X.Y. *et al.* Detection of chromosome 6 abnormalities in melanoma cell lines by chromosome arm painting probes. *Cancer Genet Cytogenet* 107, 89-92 (1998).

55. Lee, J.J. *et al.* Targeted next-generation sequencing reveals high frequency of mutations in epigenetic regulators across treatment-naive patient melanomas. *Clin Epigenetics* 7, 59 (2015).
56. Shain, A.H. *et al.* Exome sequencing of desmoplastic melanoma identifies recurrent NFKBIE promoter mutations and diverse activating mutations in the MAPK pathway. *Nat Genet* 47, 1194-9 (2015).
57. Saito, Y. *et al.* Endogenous melanin-concentrating hormone receptor SLC-1 in human melanoma SK-MEL-37 cells. *Biochem Biophys Res Commun* 289, 44-50 (2001).
58. Cifola, I. *et al.* Comprehensive genomic characterization of cutaneous malignant melanoma cell lines derived from metastatic lesions by whole-exome sequencing and SNP array profiling. *PLoS One* 8, e63597 (2013).
59. Zhang, J.P. *et al.* Notch ligand Delta-like 1 promotes the metastasis of melanoma by enhancing tumor adhesion. *Braz J Med Biol Res* 47, 299-306 (2014).
60. Wiesner, T. *et al.* Kinase fusions are frequent in Spitz tumours and spitzoid melanomas. *Nat Commun* 5, 3116 (2014).
61. Ray, M.E., Su, Y.A., Meltzer, P.S. & Trent, J.M. Isolation and characterization of genes associated with chromosome-6 mediated tumor suppression in human malignant melanoma. *Oncogene* 12, 2527-33 (1996).
62. Laurette, P. *et al.* Transcription factor MITF and remodeller BRG1 define chromatin organisation at regulatory elements in melanoma cells. *Elife* 4(2015).
63. Aktary, Z., Corvelo, A., Estrin, C. & Larue, L. Sequencing two Tyr::CreER(T2) transgenic mouse lines. *Pigment Cell Melanoma Res* (2019).
64. Gallagher, S.J. *et al.* General strategy to analyse melanoma in mice. *Pigment cell & melanoma research* 24, 987-8 (2011).
65. Robinson, M.D., McCarthy, D.J. & Smyth, G.K. edgeR: a Bioconductor package for differential expression analysis of digital gene expression data. *Bioinformatics* 26, 139-140 (2010).
66. Ritchie, M.E. *et al.* limma powers differential expression analyses for RNA-sequencing and microarray studies. *Nucleic acids research* 43, e47 (2015).
67. Chen, E.Y. *et al.* Enrichr: interactive and collaborative HTML5 gene list enrichment analysis tool. *BMC Bioinformatics* 14, 128 (2013).
68. Bennett, D.C., Cooper, P.J. & Hart, I.R. A line of non-tumorigenic mouse melanocytes, syngeneic with the B16 melanoma and requiring a tumour promoter for growth. *International journal of cancer* 39, 414-8 (1987).
69. Strub, T. *et al.* Essential role of microphthalmia transcription factor for DNA replication, mitosis and genomic stability in melanoma. *Oncogene* 30, 2319-32 (2011).
70. Ghanem, G.E., Comunale, G., Libert, A., Vercammen-Grandjean, A. & Lejeune, F.J. Evidence for alpha-melanocyte-stimulating hormone (alpha-MSH) receptors on human malignant melanoma cells. *Int J Cancer* 41, 248-55 (1988).
71. Rambow, F. *et al.* New Functional Signatures for Understanding Melanoma Biology from Tumor Cell Lineage-Specific Analysis. *Cell Rep* 13, 840-53 (2015).

72. Petit, V. *et al.* C57BL/6 congenic mouse NRAS(Q61K) melanoma cell lines are highly sensitive to the combination of Mek and Akt inhibitors in vitro and in vivo. *Pigment Cell Melanoma Res* (2019).

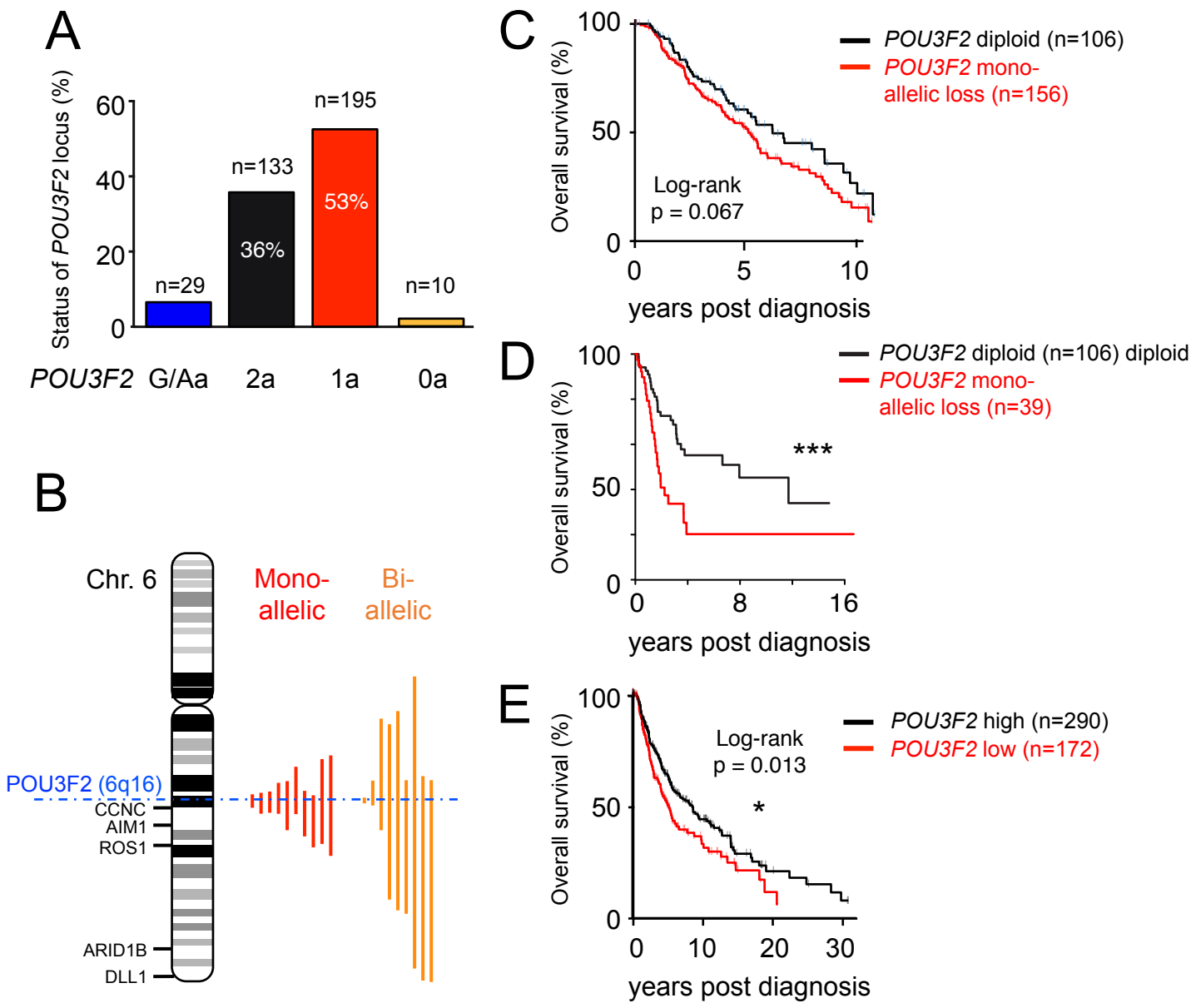

Figure 1

Hamm et al

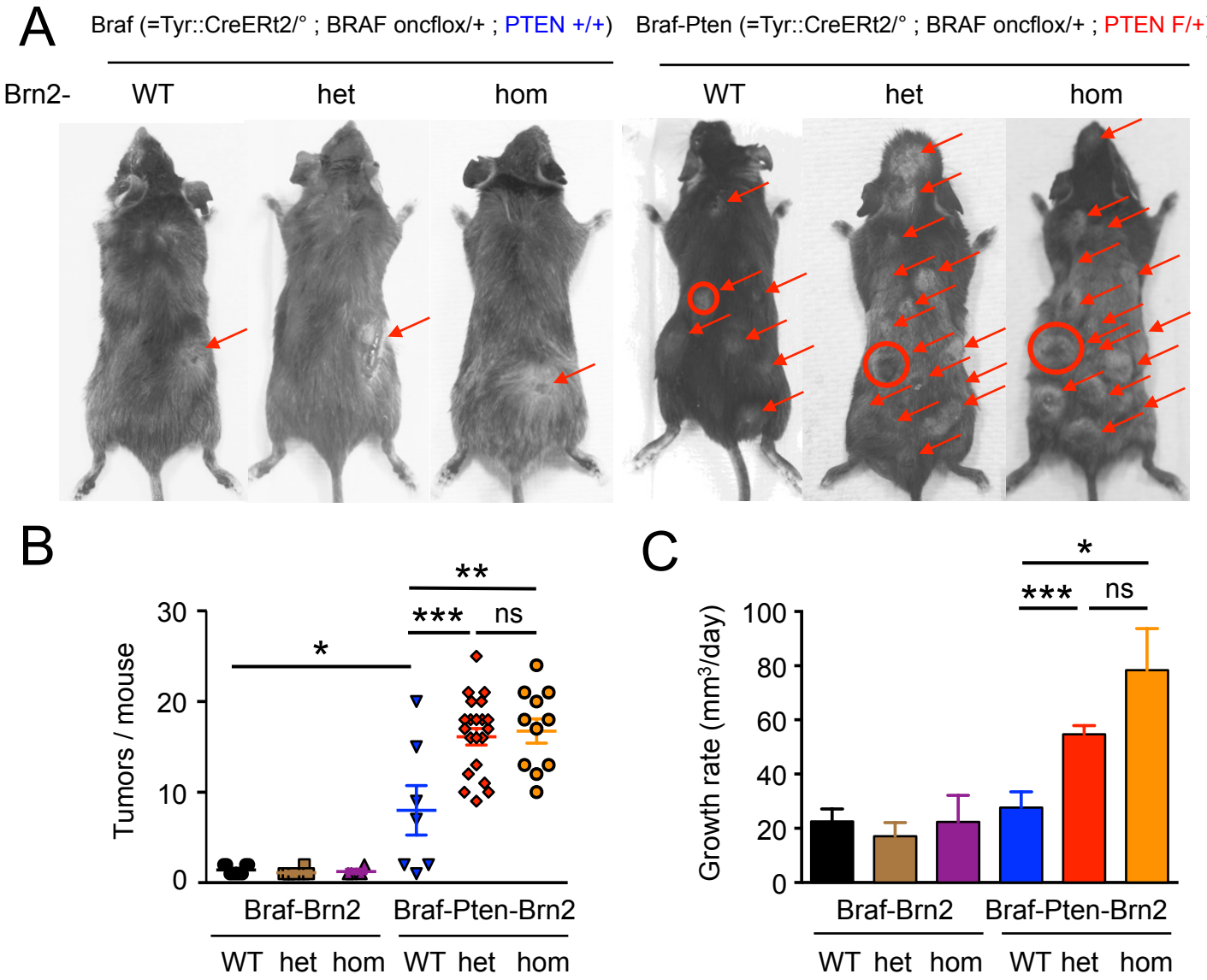

Figure 2

Hamm et al

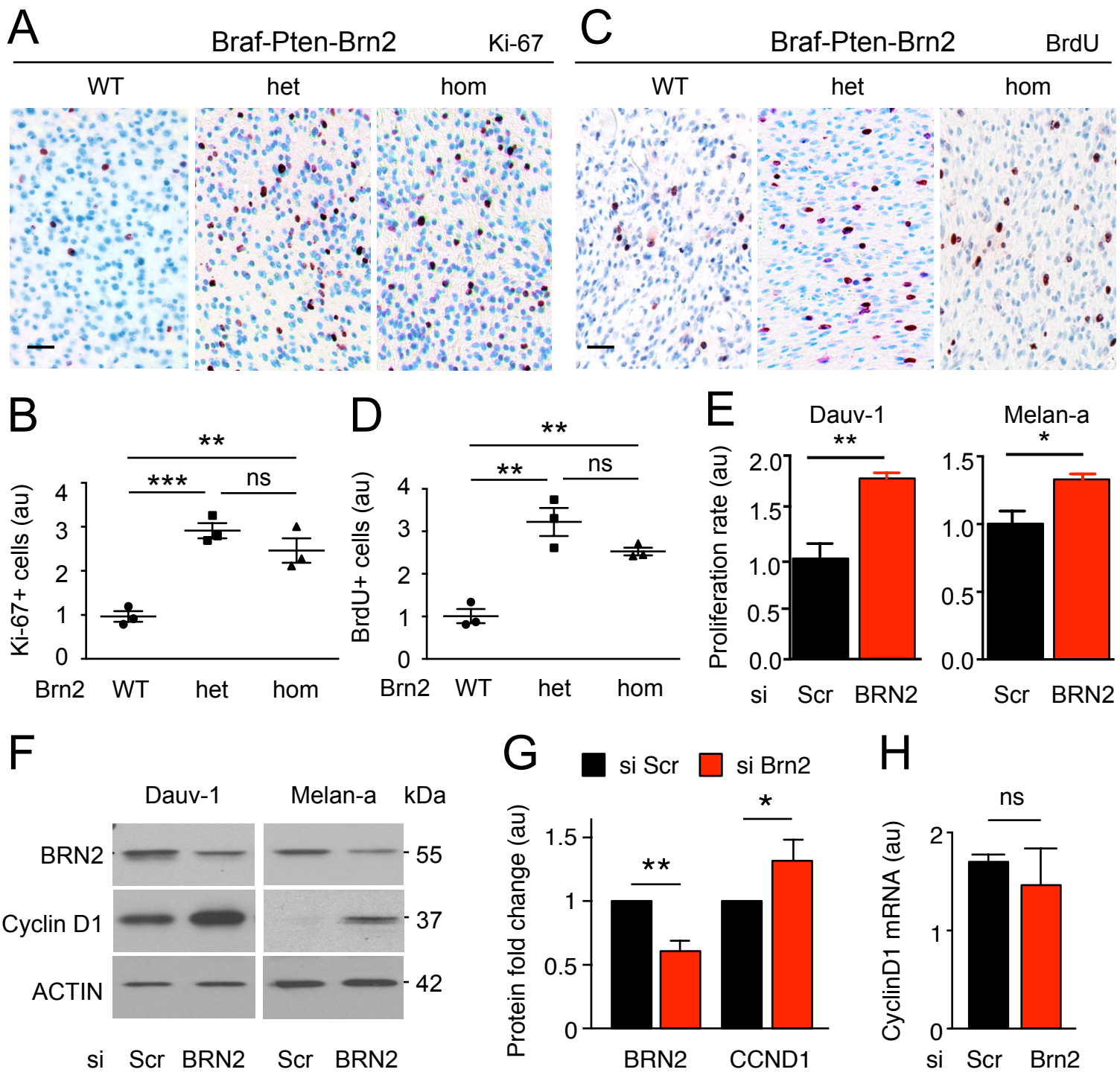

Figure 3

Hamm et al

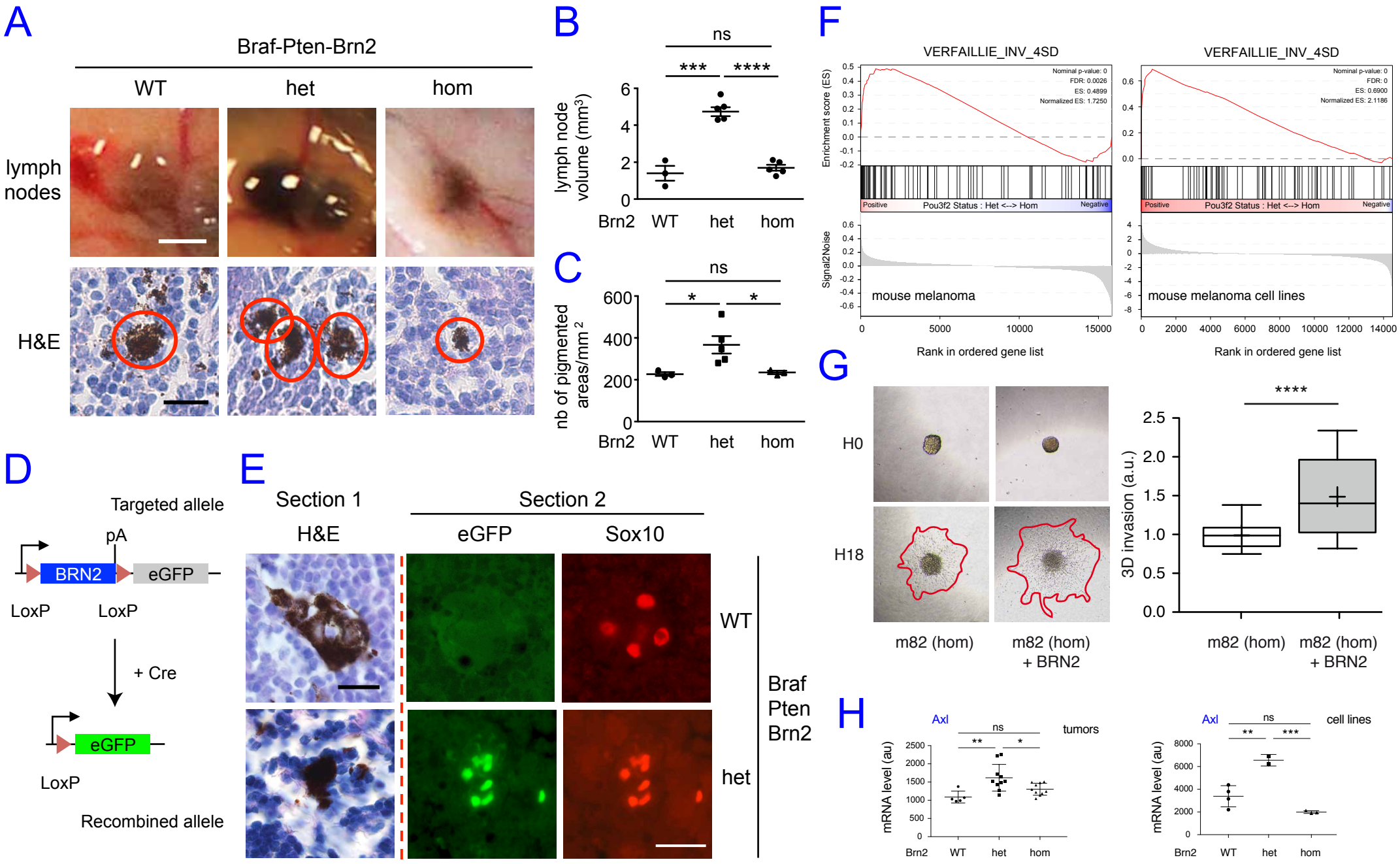

Figure 4

Hamm et al

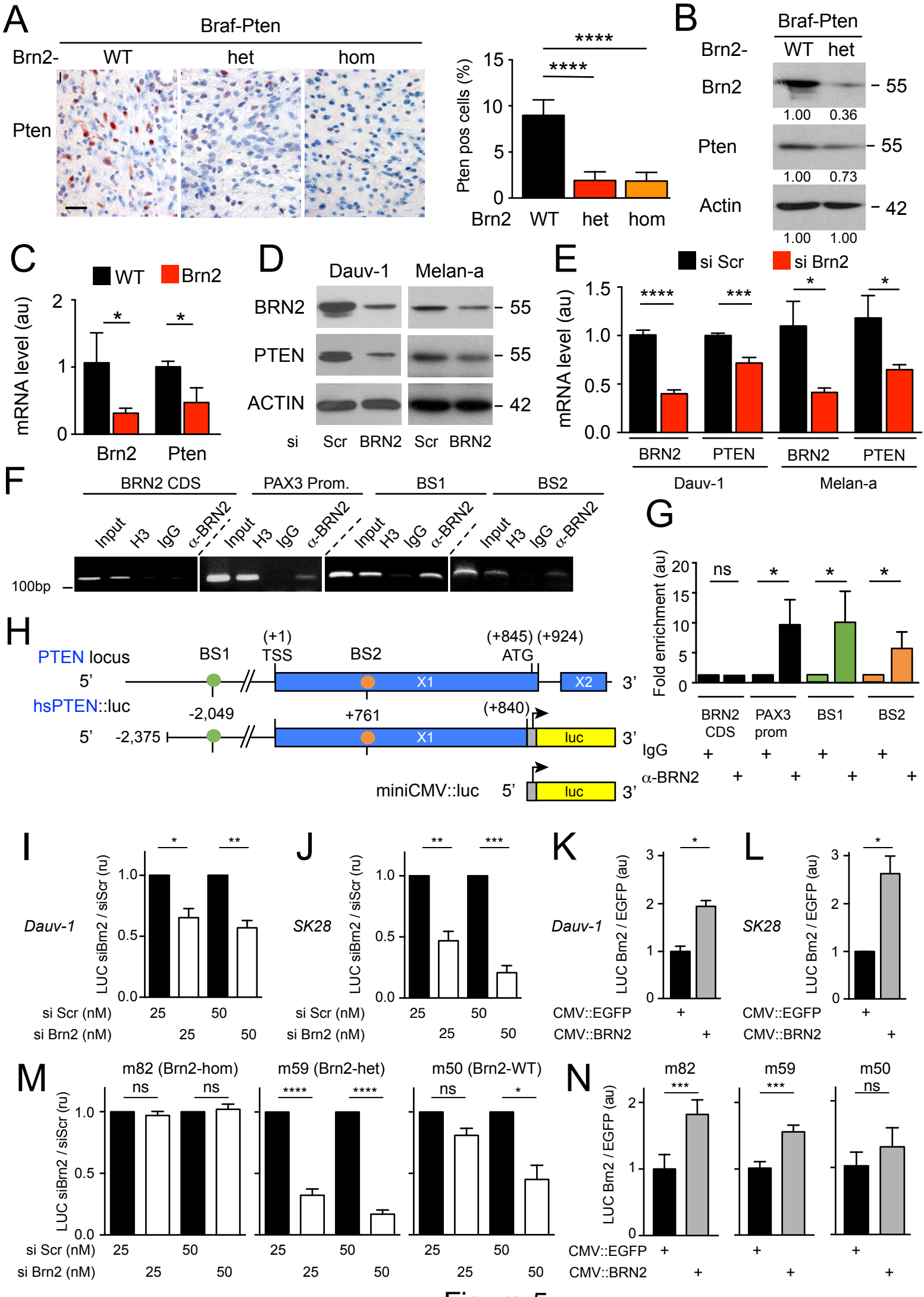

Figure 5

Hamm et al

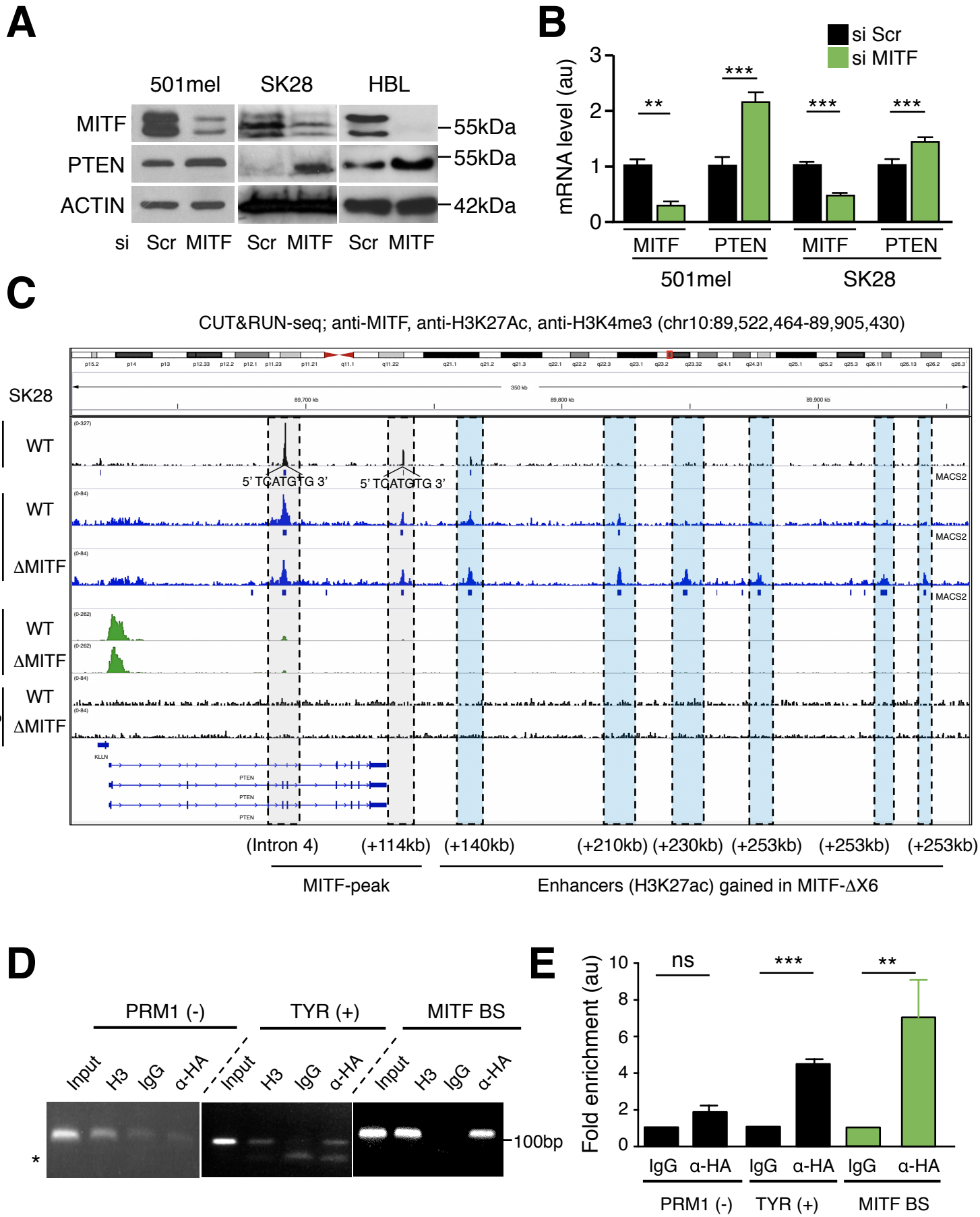

Figure 6

Hamm et al